Pseudomonas aeruginosa resistance of monosaccharide-functionalized glass surfaces

Mathieu Scalabrini, Jonathan Hamon, Isabelle Linossier, Vincent Ferrières, Karine Réhel

Pseudomonas aeruginosa resistance of monosaccharide-functionalized glass surfaces

Mathieu Scalabrini [a,*], Jonathan Hamon [c], Isabelle Linossier [a], Vincent Ferrières [b,*] and Karine Réhel [a]

[a]Univ Bretagne-Sud, EA 3884, LBCM, IUEM, F-56100 Lorient, France.
[b]Univ Rennes, Ecole Nationale Supérieure de Chimie de Rennes, CNRS, ISCR – UMR6226, F-35000 Rennes, France.
[c]Institut des Matériaux Jean Rouxel (IMN), Université de Nantes, CNRS UMR6502, Institut des Matériaux Jean Rouxel, 2 rue de la Houssinière, BP32229, Nantes Cedex 3 44322, France

*Corresponding authors.
E-mail address: M. Scalabrini (scalabrini.mathieu@gmail.com), V. Ferrières (vincent.ferrieres@ensc-rennes.fr)

This manuscript is composed of 7817 words with 6 figures and 2 tables

Highlight

- Amphiphilic monocarbohydrate surfaces are designed with D-glucose, D-galactose and D-mannose
- Adhesion of *Pseudomonas aeruginosa* is reduced by 40% with simple carbohydrate layer
- The adhesion resistance is dependent on physicochemical properties of the carbohydrates, rather than molecular interactions.

Abstract

Preventing microorganism colonization on a surface is a great challenge in the conception of medical, food and marine devices. Here, we describe the formation of carbohydrate functionalized glass surfaces with D-glucose, D-galactose and D-mannose and how they efficiently affected the bacterial attachment. The carbohydrate entities were covalently attached to the pre-functionalized surface by click chemistry thanks the copper catalysed alkyl-azide cycloaddition. Water contact angle and X-ray photoelectron spectroscopy characterisations showed a homogeneous and quantitative cycloaddition at the scale of

microorganisms. The adhesion assays with *Pseudomonas aeruginosa*, used as model of opportunistic pathogen, indicated a significant diminution of almost 40% of the bacterial accumulation on glycosidic surfaces with respect to initial surface. This activity was further compared with a surface presenting a simple hydroxyl residue. Exploration of specific interactions through Lectin A deficient *Pseudomonas aeruginosa* mutant strain provided new evidences that Lectin A was involved in biofilm maturation, rather than bacterial attachment. Subsequently, the determination of surface free energy and the adhesion free energy between surfaces and bacterial cell wall showed that the adhesion was thermodynamically unfavourable.

Keywords: *surface, functionalization, carbohydrate, bacterial adhesion, Pseudomonas aeruginosa*

1. Introduction

Biofilm is a bacterial organized community strongly held on live or abiotic surfaces in aqueous media. Bacteria are maintained to each other by excreting a matrix of extracellular polymeric substances (EPS) composed mainly of polysaccharides, proteins and DNA. The high viscosity of the matrix protects the bacteria at the centre of biofilm from environment, chemical and/or thermic treatment and immune system, and enhances the bacterial tolerance against anti-bacterial drugs [1,2].

Biofilms occur in many different fields, resulting in major health and economic issues. *Pseudomonas aeruginosa*, *Escherichia coli, Staphylococcus epidermidis* or *Staphylococcus aureus* are such bacteria adept in forming biofilms on many medical devices from urinary and venous catheters to dental and orthopaedic implants. They consequently cause health complications with nosocomial infections and diseases, that can be fatal mainly with immunodeficiency persons [2–5]. Furthermore, in addition to accelerate the corrosion and the maintenance frequency of equipment, biofilms on food contact surfaces minimize the effect of cleaning agents, and thus increase the odds of food contaminations by *Listeria monocytogenes* or *Salmonella* which, in most cases, trigger potentially fatal foodborne disease [6–9]. Lastly, marine structures such as ships, underwater pipelines, oil rings are continually in contact with water that are profitable to the development of biofouling. This increases the downside risks and the rhythm of cleaning and maintenance processes and then results in substantial economic losses [10,11].

Biofilm formation is a complex process not clearly elucidated but it is recognized to be subdivided in sequential steps [12,13]. Firstly, planktonic bacteria reversibly adhere onto the surface with weak interactions such as van der Waals interactions, electrostatic interactions and hydrogen bonds. This step is immediately followed by an irreversible attachment of the

bacteria thanks to a primary excreted film and flagella, pili and some other membrane structures including lectins [14,15]. Then, bacteria progressively grow in microcolonies leading up to more structured and condensed architectures. After maturation, almost all the area is colonized, and a part of sessile bacteria finally returns in planktonic state to colonize other surfaces. The accumulation of microbial mass on the surface can be limited and disrupted by interfering at one or more stages of the biofilm formation. Antimicrobial or biocidal coatings are the most powerful against biofilm formation [16,17]. Nonetheless, using bactericidal strategy may induce dangerous consequences, especially in health domain, with the rising of multi-resistant bacteria, resulting from the abuse and misuse of drugs.

A non-biocidal and non-toxic strategy to prevent bioaccumulation lies in the development of surfaces with adhesion resistance properties. One effectiveness approach to prevent microorganism accumulation is the use of amphiphilic copolymers such as silane-PEG which demonstrated a good fouling release properties in complex environment [18,19]. PEG chains form a hydrated layer that creates a steric barrier preventing close approach of microorganisms as well as unspecific interactions. Indeed, when bacteria enter in contact of PEG entities, the layer is compressed increasing the osmotic pressure that leads to repulsive force against bacteria [20,21]. PEG brush-coated nevertheless have a limited *in vivo* stability over time increasing research of PEG brush-like substitutes [22,23].

Carbohydrates are biocompatible and non-toxic compounds with numerous functional groups affording an extensively possibility of structural and property modulations. Moreover, chitosan, alginate, hyaluronic acid and dextran are some of polysaccharides described for their ability to minimise protein adsorption, fouling attachment and biofilm formation [24–27]. Exopolysaccharides isolated from EPS matrix have also been shown to negatively regulate biofilm formation (see Rendueles [28] for an extensive summary). Hederos and co-workers presented surfaces designed from self-assembled monolayer of partially methylated galactosides which resisted to the adsorption of proteins [29]. Recent studies on marine bacteria and *Ulva linza* macroalgae have shown to curtail the adhesion on one side and to aid the cleaning on the other side [30]. *In vivo* studies of immobilized lactose on poly(ether sulfone) (PES) revealed detrimental effects on both protein adsorption and biomass accumulation [31]. Valotteau has demonstrated that a sophorolipide-functionalized surface (SL) possessed antibacterial properties by destabilizing the cell wall of bacteria [32]. Further studies by single-cell force spectroscopy showed an inhibition of the bacterial adhesion force with SL surfaces [33]. These latter studies strongly suggest that surface-immobilized mono- or disaccharides may impact the bioaccumulation even if, to the best of our knowledge, they are still underexplored on pathogenic bacteria.

Based on mechanism from PEG units and proprieties from carbohydrates, this work explores the anti-bioadhesion activities of amphiphilic monosaccharides layer grafted on glass

surface. D-glucose (D-Glc), D-galactose (D-Gal) and D-mannose (D-Man) were simply connected to pre-functionalized alkyl azide glass through a small propargylic linker thanks to copper catalysed alkyne-azide cycloaddition (CuAAC). It is noteworthy that triazole rings were sometimes able to mimic carbohydrate residues that results in virtual increase of the glycosidic chain length [34,35]. Two type of linkage were explored, the standard *O*-glycosidic bonds and *S*-glycosidic linkages, the latter being more resistant to chemical and enzymatic hydrolysis [36,37]. The glycosidic surfaces were further compared to hydroxylated surface, which bears the triazolic linker terminated by a hydroxyl group which closely akin to glycosidic surface (**Figure 1**). The resulting surfaces were then characterized by water contact angle and X-ray Photoelectron Spectroscopy (XPS). Adhesion assays were performed with opportunistic pathogen *Pseudomonas aeruginosa* by means of parallel plate flow chamber system. Adhesion results are discussed in terms of specific interaction and unspecific interaction by examining the adhesion change with lectin A deficient mutant as well as the surface free energies and the thermodynamic Lifshift-van der Waals – Acid-Base (LW-AB) approach.

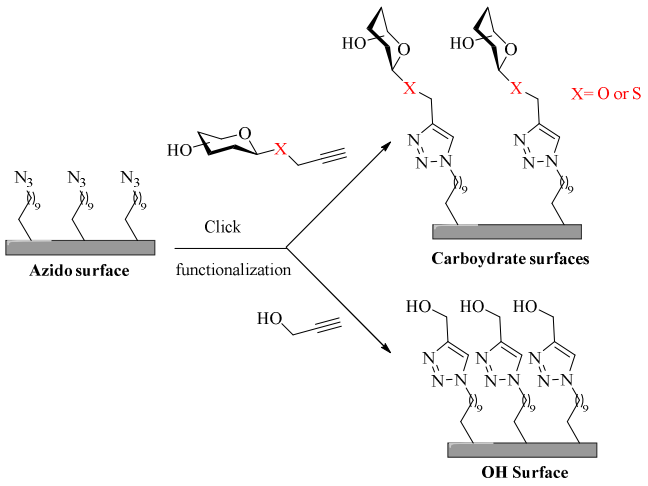

Figure 1. Principle and design of monocarbohydrate-functionalized surfaces.

2. Materials and methods

2.1. Chemicals and materials

All reagents and solvents were purchased from commercial sources and were used without further purification unless noted. Unless otherwise stated, all reactions were monitored by TLC on Silica Gel 60 F 254. TLC spots were detected by staining with cerium ammonium molybdate solution. Column chromatography was performed on Silica Gel (50 µm). NMR spectra were recorded on Bruker ARX 400 spectrometer at 400 MHz for ^{1}H and 100 MHz for ^{13}C. Chemical shifts are given in δ units (ppm) and referenced to TMS. Coupling constants J were calculated

in Hertz (Hz). Proton and carbon NMR peaks were unambiguously assigned by J-Mod (J-Modulated spin echo), COSY (double quantum filtered with gradient pulse for selection), HSQC (gradient echo-anti-echo selection and shape pulse) and HMBC (echo-anti-echo gradient selection, magnitude mode) correlation experiments. Alkyl azide-functionalized glass surfaces were purchased from PolyAn – Molecular Surface Engineering (Germany).

2.2. Bacterial strain

Pseudomonas aeruginosa wild-type MPAO1 and mutant PAΔ*lecA* (ref: PW5314 lecA-G10::ISphoA/hah) provided from Two-Allele Library Manoil lab (University of Washington).[38] Syto™ 9 Green were purchased on Fisher scientific. Cell were routinely cultivated at 37 °C in LB medium (NaCl 10 g/L, Tryptone 10 g/L, Yeast extract 5 g/L) under agitation (120 RPM).

2.3. Synthesis of Propargyl *O*-D-glycopyranosides 2a-2c

To a solution of peracetylated sugar (1.0 equiv.) in dry CH_2Cl_2 was subsequently added $BF_3.OEt_2$ (1.5 equiv.) and propargyl alcohol (1.5 equiv.) under inert atmosphere (N_2). The reactional mixture was stirred overnight at room temperature and the reaction was quenched with K_2CO_3 (1.5 equiv.). After stirring another 1 hour, the mixture was filtered on Büchner and the filtrate was diluted in CH_2Cl_2, washed with H_2O (2x) and brine solution (1x). The organic layer was dried over $MgSO_4$, filtered and concentrated under reduced pressure to yield the desired product directly used without further purification.

To a solution of propargyl 2,3,4,6-tetra-*O*-acetyl-β-D-glycopyranoside (1.0 equiv.) in CH_3OH/H_2O (6:1) was added Et_3N (4.5 equiv.). The reaction was allowed to stir at 20 °C until complete deprotection monitored by TLC [CH_2Cl_2/CH_3OH (9:1)]. The mixture was concentrated, and the product was isolated by flash chromatography on silica gel with CH_2Cl_2/CH_3OH (9:1) as eluent. The detailed characterization of compounds is given in Supplementary Information.

2.4. Synthesis of Propargyl 1-thio-D-glycopyranosides 4a-4c

To a solution of peracetylated sugar (1.0 equiv.) in dry CH_3CN were added thiourea (1.1 equiv.), $BF_3.OEt_2$ (3.0 equiv.) and the reactional mixture was stirred under reflux for 1 hour. After reaching room temperature, propargyle bromide (1.5 equiv., 80%w in toluene) and Et_3N (4.5 equiv.) were slowly added and then, the reaction mixture was stirred at 20 °C for 12 hours. After completion, the mixture was concentrated, the resulting paste was diluted in CH_2Cl_2, washed with HCl 5% (2x), brine solution (3x) and distilled water (2x). The collected organic layer was dried over Na_2SO_4, filtered and concentrated under reduced pressure at 40 °C. The

residue was finally purified by flash chromatography on silica gel using an eluent gradient of cyclohexane/EtOAc (4:1 to 1:1) to yield the desired product.

To a solution of propargyl 2,3,4,6-tetra-*O*-acetyl-1-thio-β-D-glycopyranoside (1.0 equiv.) in CH_3OH/H_2O (6:1) was added Et_3N (4.5 equiv.). The reaction was allowed to stir at 20 °C until complete deacetylation monitored by TLC [CH_2Cl_2/CH_3OH (9:1)]. The mixture was further concentrated, and the product was isolated by flash chromatography on silica gel eluting with CH_2Cl_2/CH_3OH (9:1). The detailed characterizations of compounds are given in Supplementary Information.

2.5. Grafting protocol

Commercially available alkyl azide-functionalized glass surfaces (75x25x1 mm) were immersed in a solution of H_2O/DMSO (1:1). Propargyl glycopyranoside (2.3 mM) and $CuSO_4.5H_2O$ (1.2 mM) were added and oxygen was removed from the mixture by bubbling with N_2 for 20 min. Then, sodium ascorbate (2.3 mM) was added and the mixture was bubbling for another 15 min. The reactor was kept in the dark and incubated at 35 °C under agitation for 48 h. The resulting grafted surfaces were thoroughly washed with H_2O and absolute EtOH and dried in hoven at 40 °C. Finally, grafted surfaces were kept at -20 °C prior to further use.

2.6. Contact angle and surface free energy

Water drop contact angles were measured with the optical contact angle meter Digidrop (GBX). A drop of 1.5 μL of ultra-pure water at 20 °C was deposited on the surfaces and the profile was recorded. Contact angle was determined from the analysis of the drop shape with the instrument software. The presented contact angles of each surfaces are averaged from ten surfaces from different batches, and six measurements were made on each surface. The determination of surface energy components was achieved using water and formamide as polar solvent and diiodomethane as apolar solvent with known data (values are presented in Table S1).

2.7. XPS Analysis

X-ray photoelectron spectroscopy analysis was performed using a Kratos Axis Nova (University of Nantes, France). The spectrometer used a monochromated Al Kα source (1486.6 eV) operating at 300W (20 mA, 15 kV) and an analysis area of 700 μm x 300 μm. The pressure in the analysis chamber was always kept below 10^{-9} Torr. High-resolution spectra of different core levels were recorded using a pass energy of 40 eV at $\theta = 0°$ take-off angle (angle between the surface normal and the detection direction). All data were acquired using charge compensation to establish a steady state surface potential. All high-resolution spectra were

analyzed and fitted using CasaXPS software. All spectra were calibrated in energy by setting adventitious carbon C 1s at 284.8 eV (binding energy). All spectra were fitted using a Tougaard type baseline for the background and a pseudo-Voigt function with Gaussian (70%)-Lorentzian (30%) for each component.

2.8. Characterization of MPAO1 cell wall

Culture of MPAO1 were carried out at 37 °C in 100 mL of LB medium under agitation (120 RPM). Cells were harvested by ultra-centrifugation, washed (3x) and suspended in physiological water (NaCl 0.9%) at a concentration of 3×10^9 cell/mL. 50 mL of the bacterial suspension were filtered through 0.45 μm pore size filters. Filters were placed on a glass slide and left to air dry for 30 min at 37 °C.[39,40] Finally, a droplet of 1.5 μL of desired solvents (water, formamide and diiodomethane) was deposited on the filter and contact angle was measured after 2 seconds. Two measurements by filters were achieved from three independent experiments.

2.9. Bioadhesion assays

Bacterial adhesion was carried with a flowcell system under static condition. Flowcell was composed of 3 independent channels (40x4x1 mm). The surface was stuck onto the flowcell with silicon glue and connected to a peristaltic pump. The system was sterilized with a flow of absolute ethanol for at least 1 hour. Then, the system was washed and equilibrated with physiological water. Each channel was inoculated with a 300 μL of suspension of the desired strain at OD_{600}= 0.1 in physiological water and bacteria were allowed to adhere to the surface at 37 °C for two hours. Non-adhered bacteria were removed with a minimal flow and adhered bacteria were stained with a solution of 5 μM of Syto™ 9 Green, a nucleic live/dead cell stain ($\lambda_{excitation}$= 485 - 486 nm, $\lambda_{emission}$= 498 – 501 nm). After 15 min in the dark, five points of view were taken on each channel with an inverse laser scanning confocal microscopy (Zeiss, LSM 710, Oberkochen, Germany) with an in-air 40x objective. Resulting pictures were converted to binary ones and the surface coverage rate was determined from the black and white pixels ratio with the open access software ImageJ. Finally, the average-to-average statistical comparisons of five independent adhesion assays were determined by Analysis of Variance (ANOVA) with Tukey HSD test.

3. Results and discussion

3.1. Synthesis and surface functionalization

D-Glucose, D-galactose and D-mannose are the most abundant carbohydrates that play crucial roles in life such as in structural role, cell-cell interactions or in the regulation of genes. Their multiple hydroxyl functions are very attractive for elaborating material through easy modulation of physicochemical properties. *S*/*O*-D-Glucopyranosidic (*S*/*O*-Glc*p*), *S*/*O*-D-galactopyranosidic (*S*/*O*-Gal*p*) and *S*/*O*-D-mannopyranosidic (*S*/*O*-Man*p*) surfaces were obtained by "clicking" propargyl glycosides on commercially alkyl azide-functionalized glass plates. The facility and the high selectivity in a wide range of solvent and temperature make the CuAAC reaction, the most used "click" reaction in organic chemistry and materials. *S*/*O*-Propargyl D-glycosides were already synthesised and described from commercially available peracetylated glycosides in two steps (**Figure 2**). They were obtained by Lewis acid catalysed glycosylation of propargyl alcohol from the desired peracetylated monosaccharide with complete 1,2-*trans* diasteroselection. Then, acetyl groups were removed under Zemplén basic conditions. ^{1}H NMR spectra showed characteristic signals in accordance with previous published data [41]. In the case of propargyl *S*-glycopyranosides, it was interesting to find a pathway to stave off the risk of the foul odour and toxicity of thiol compounds. In this way, **4a-4c** were synthesised in two steps from roots of Ibatullin [42,43] giving access to derived *S*-glycosides in one-pot procedure. Briefly, a glycosyl isothiuronium salt was formed *in situ* from a peracetylated carbohydrate. The latter intermediate was allowed to react with propargyl bromide in the presence of trimethylamine. The resulting products **3a-3c** were subsequently deprotected by transesterification to afford the desired thioglycosides **4a-4c**. All compounds and their intermediates were characterized by 1D NMR and obtained data are similar to the literature [44–46].

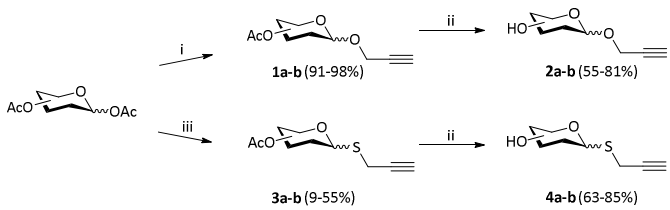

Figure 2. General procedure for the synthesis of *O*- and *S*-propargylated glycosides from peracetylated D-glucoside (**a**), D-galactoside (**b**) and D-mannoside (**c**). i) Propargyl alcohol, $BF_3.OEt_2$, DCM, overnight, r.t.; ii) Et_3N, H_2O/MeOH, 20 °C; iii) Thiourea, $BF_3.OEt_2$, MeCN, reflux then propargyl bromide, Et_3N, r.t.

The glycosylated glass surfaces were obtained by grafting the propargyl monosaccharides to the azide group pre-installed on the material, using usual conditions of CuAAC (**Figure 3**) [47,48]. Azide surface was immersed in a solution of the desired carbohydrate **2a-2c** or **4a-4c**, copper sulphate and sodium ascorbate in dimethyl sulfoxide and water. The reaction was incubated at 35 °C in the dark for 48 hours. To remove the copper outstripped, glycosidic surfaces were thoroughly washed with water and ethanol. A similar procedure was applied to the simpler surface presenting only hydroxyl group, starting from propargyl alcohol (OH surface).

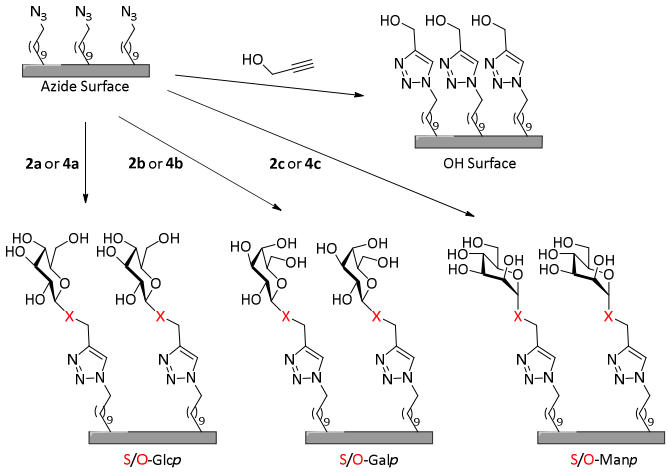

Figure 3. Grafting pathway of glycosides **2a**-**c** and **4a**-**c** on commercial azide-functionalized glass surface.

3.2. Water Contact Angle

The evolution of the wettability property of the surfaces throughout the different grafting was characterized by the contact angle of a water droplet. The measurement was performed on ten surfaces from different reaction batches and the mean values are reported in Figure 4.

The reference azide surface displayed the most hydrophobic character with an angle values up to 76° ± 2° within the range of value already cited in the literature (77°) [49]. Modification with a simple hydroxyl group enhanced the water affinity of the OH surface with a weak decrease of the hydrophobicity (contact angle 68° ± 2°). Surprisingly, the angle exhibited by OH was higher than angle previously determined on OH-terminated gold surfaces (average 30°) [50]. A difference in the grafting density and the functionalization method might explain the large gap. However, the contribution of the multiple hydroxyl groups of carbohydrates led to an expected decrease of the water contact angle with values lied between 56° ± 2° and 58° ± 2°. Thereover, the similar angle for glycosidic layer indicated that the nature of the sugar and the glycosidic linkage had thus no impact on the hydrophilicity. And the similarity of standard

deviations before and after cycloaddition implied a homogeneous functionalization at the organism scale.

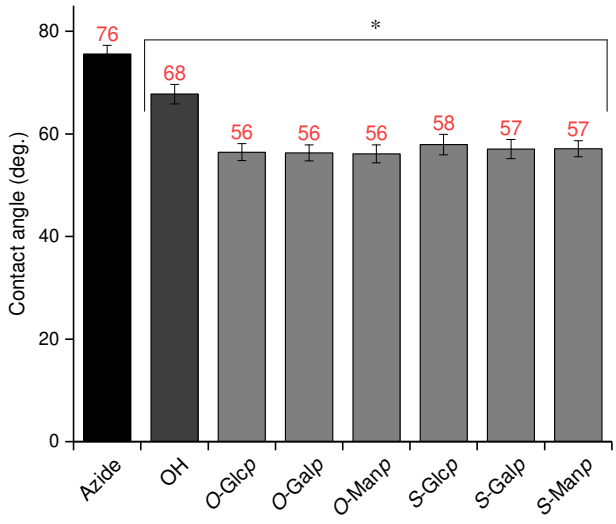

Figure 4. Contact angle of a water droplet deposited on the surfaces. The values are the means of six measurements on ten surfaces from independent batches. * indicates a significant difference at $p < 0.01$ with respect to azide surface (ANOVA).

3.3. X-Ray photoelectron spectroscopy

The cycloaddition reaction was corroborated with the in-depth XPS analysis of atomistic composition change of the surfaces. First of all, information from large spectrum on different surfaces validated the absence of residual copper which could be prejudicial for biological studies (**Figure S1**). Secondly, the characteristic double signal in the N 1s high resolution scan of azide surface (**Figure 5a**) was deconvoluted into three peaks: 404.5 eV and 400.0 eV attributed to the azide group (electron-deficient nitrogen $^{-}$N=**N**$^{+}$=N- and the two lateral nitrogen $^{-}$**N**=N^{+}=**N**-, respectively) and one at 401.0 eV assigned to NH_2/NH_3^+ resulting from the known photolytic degradation of the azide group [49,52,53]. Figure 5b and Figure S2 show the typical N 1s spectra for functionalized surfaces. The broaden signal at 400 eV was fitted and deconvoluted in two peaks: 402.2 eV and 400.1 eV assigned to the triazole ring (**N**-N=N and N-**N**=**N**, respectively). As expected, the calculated ratio of area under the peaks was 1:2 for grafted surfaces. Finally, the absence of 404.5 eV signal provided evidence that the cycloaddition “click” reaction was nearly quantitative.

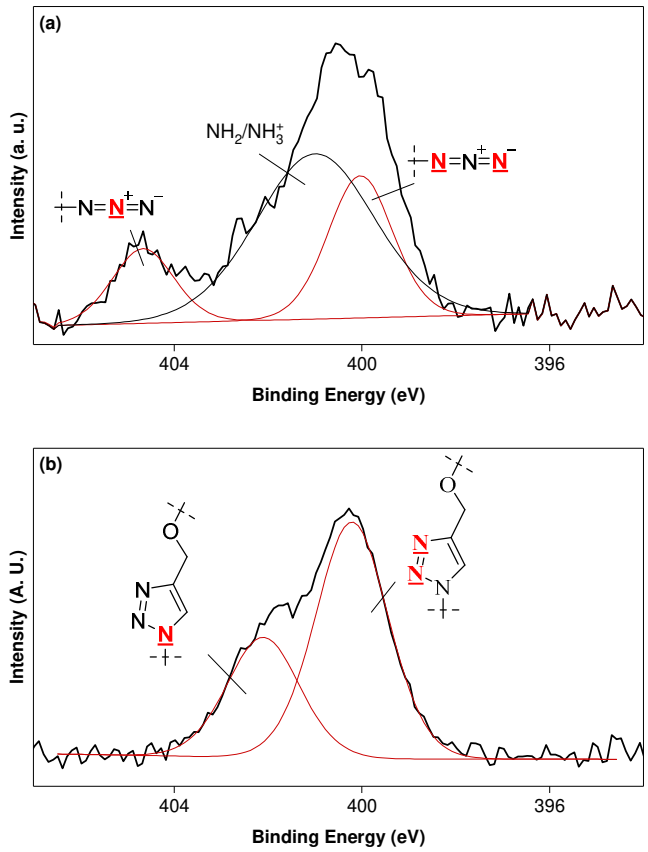

Figure 5. XPS narrow scans of the N 1s region of azide-functionalized surface (**a**) and *O*-Glucose functionalized surface (**b**). After the cycloaddition, the initial double signal disappeared to give one broaden signal.

3.4. Bioadhesion Assays

The Gram-negative *Pseudomonas aeruginosa* is an opportunistic pathogen involved in nosocomial and chronic lung infections [54–56]. In most cases, this type of infections is due to a transfer from contaminated devices to the host. Plethora of literature data on its ability to form biofilm on biotic and abiotic surfaces makes *P. aeruginosa* a reference in the area. The bacterial adhesion is mostly dependent on hydrophobicity and surface charge of both the surface and the bacterium, and can be described with the Derjaguin-Landau-Verwey-Overbeek (DLVO) model for colloidal particles [57,58]. Once initial adhesion, bacteria are strongly anchored to the surface thanks to the excreted EPS and specific interactions through membranes structures such as lectins [14,59].

The adhesion studies were performed with a flow chamber system under static condition at 37 °C. Bacteria were suspended in physiological water, a free-nutriment medium that forced the passage from the planktonic state to the sessile state and limited bacterial growth. The adhered bacteria were subsequently labelled with a solution of Syto 9 Green, snapshots were

taken using an inverse scanning laser confocal microscope; and the surface coverage rates were determined from black and white pixel ratio.

From the microscopy images presented in **Figure 6a** and **Figure S3**, the adhesion of *P. aeruginosa* was homogeneous on all surfaces with visually greater coverage for azide surface, followed by OH surface. The summary of surface coverage rates on azide, OH and glycosidic surfaces are shown in **Figures 6b** (black bars). The colonization on the control azide surface was the most important with a coverage rate at 10.0 %. Addition of a hydroxyl group did not significantly influence the adhesion whereas glycosidic patterns exhibited an anti-bioadhesion activity with the bioaccumulation decrease of almost 40% of adhered bacteria, with nevertheless no difference between carbohydrates. These observations contrast with those observed with sophorolipid-functionalized gold, where no adhesive or anti-adhesive properties were detected with a large number of bacteria [32]. However, Kesel and his group noticed that D-galactose, D-mannose and D-lactose coating reduced the adhesion of *Bacillus subtilis* in same way [60]. They suggested that carbohydrates restrained the thiol-Au interaction between proteins in the bacterial cell wall and gold surface.

Even if they are close-packed, presenting carbohydrate pattern may lead to specific interactions with carbohydrate binding proteins present on the bacterial membrane [61,62]. Indeed, *P. aeruginosa* owned a soluble lectin, LecA (or PA-IL), which specifically binds α/β-D-galactosyl patterns [63,64]. Moreover, the affinity of LecA to D-galactoside is all the more important with a hydrophobic group on anomeric position [65]. Thus, bioadhesion studies were performed with the LecA deficient PAΔ*lecA* mutant in similar conditions as described for MPAO1 and the resulting coverage rates are presented in **Figure 6b** (grey bar). The coverage comparison between MPAO1 and PAΔ*lecA* indicated that the bacterial attachment was not affected in absence of LecA, even with galactosidic surfaces. It confirmed that the contribution of LecA was negligible in the adhesion step compared to their key role in the biofilm maturation [66]. Although specific interactions were not excluded, these results suggested that the adhesion of MPAO1 was dependent more on non-specific interactions (or long-range interactions) determined by the physicochemical properties of both the substratum and the bacterium.

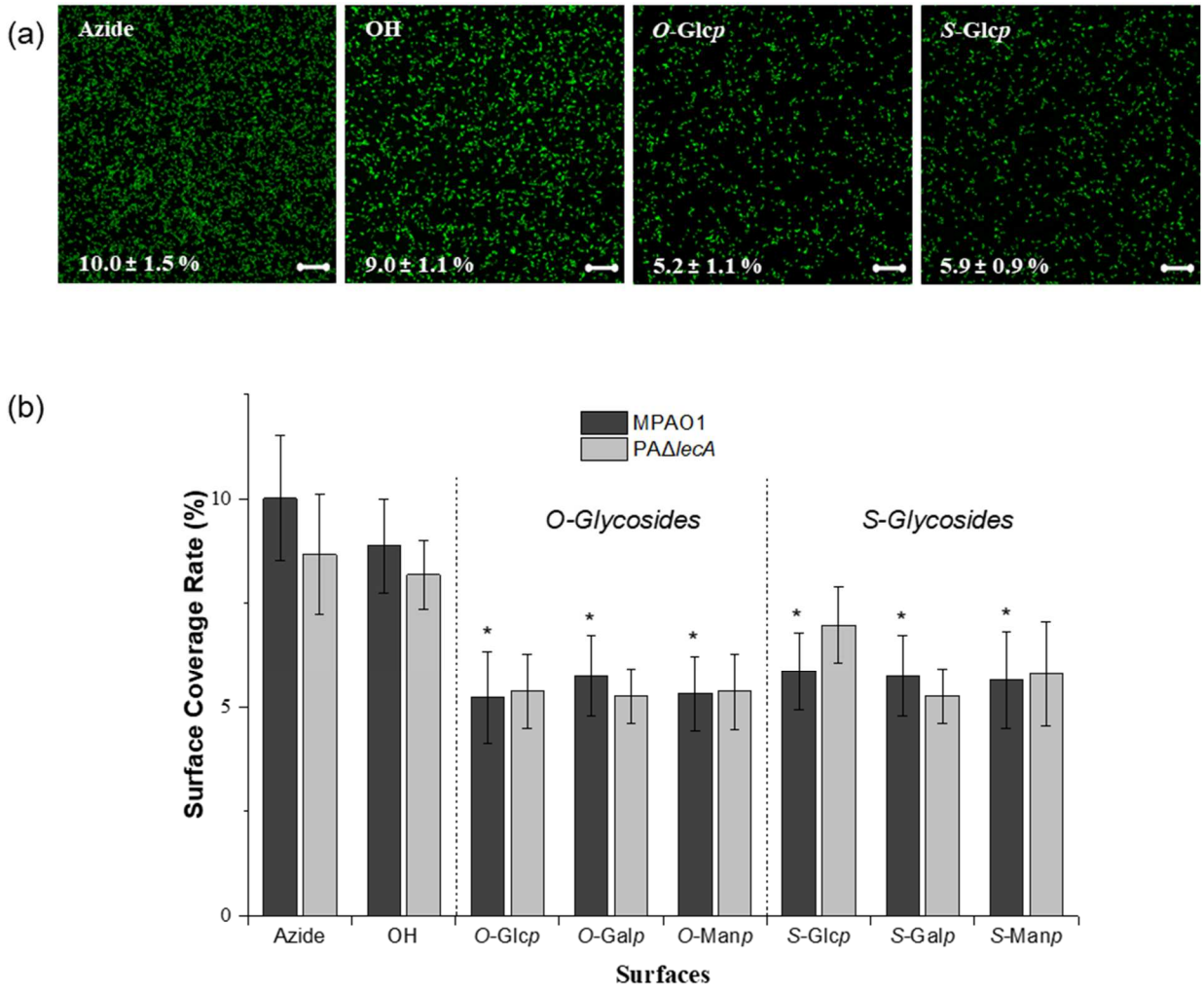

Figure 6. Qualitative and quantitative analysis of the bacterial adhesion. (a) Fluorescent confocal images of adhered MPAO1 on Azide, OH, *O*-Glc*p* and *S*-Glc*p* surfaces (Scale bar = 20 μm). (b) Surface coverage rates of MPAO1 and PAΔ*lecA*. *Significant difference with respect to azide surface ($p < 0.01$).

3.5. Surface free energy

The surface free energy (or surface tension) is an important parameter influencing the adhesion. According to the van Oss, Chaudhury and Good (VCC) theory, the surface free energy of a dipolar surface γ_s is the sum of a Lifshitz-van der Waals (dispersive) component γ_s^{LW} and Lewis acid-base (polar) component γ_s^{AB} that is depended on acid component γ_s^+ and basic component γ_s^- [67,68]:

$$\gamma_s = \gamma_s^{LW} + \gamma_s^{AB} = \gamma_s^{LW} + 2\sqrt{\gamma_s^- \gamma_s^+}$$

Following a combining rule, a general contact angle equation for a liquid *l* on a solid *s* was defined as:

$$\gamma_l(1 + cos\,\theta) = 2\left(\sqrt{\gamma_s^{LW}\gamma_l^{LW}} + \sqrt{\gamma_s^{+}\gamma_l^{-}} + \sqrt{\gamma_s^{-}\gamma_l^{+}}\right)$$

Finally, the three unknown terms for the surface γ_s^{LW}, γ_s^{+}, γ_s^{-} can be found by using one apolar solvent and two polar solvents with known γ_l, γ_l^{LW}, γ_l^{-}, γ_l^{+} and γ_l^{AB} properties (see Good [69] for a complete review).

Table 1 presents the surface free energies and the components calculated from contact angle values determined with water and formamide as polar solvents and diiodomethane as apolar one (see ESI). Similar surface free energies (γ_s = 45.48-49.99 mJ/m²) were determined for all studied surfaces with a major contribution (>90 %) of the apolar component γ_s^{LW} that was assigned to the alkyl chain initially grafted on glass surface. However, different values of γ_s^{AB} were observed, notably for the Lewis basic components. Indeed, the lowest basic component was calculated for the azide surface (γ_s^{-} = 5.19 mJ/m²) resulting from their π-electrons. The grafting of OH functions provided additional hydrogen bonds that mildly increased γ_s^{-} up to 11.00 mJ/m². Finally, we observed the largest γ_s^{AB} for glycosidic surfaces with a Lewis basic component three times bigger than azide surface (γ_s^{-} = 16.83-19.11 mJ/m²). The multiple hydrogen acceptors from OH as well as with π-electrons of triazole ring gave to the glycosidic surfaces an appreciable electron donor character. Ederth and *al.* have presented similar value of surface free energy for galactosidic surfaces (γ_s = 46.4 mJ/m²) with, nevertheless, a higher value for basic component (γ_s^{-} = 67.0 mJ/m²) [30]. It is well-known that VCC theory depends on the solvent used, especially in the determination of the acid-base contribution [70].

We also determined the surface free energy of the cell wall of MPAO1 with the VCC approach using contact angle goniometry on a bacterial lawn as described by Busscher & *al.* [40]. First of all, MPAO1 exhibited a hydrophilic character with a contact angle value at 26° ± 2° which was in range of contact angle determined for “non-adhesive” *P. aeruginosa* [71]. The interfacial free energy γ_{MPAO1} was further calculated, and a clear predominance of γ_{MPAO1}^{AB} was observed, with a high contribution of Lewis basic component (γ_s^{-} = 52.63 mJ/m²). The strong electron donor and the hydrophilic characters of MPAO1 were easily attributed to structures, such as lipopolysaccharides, lipoproteins, phospholipids and proteins, which compose the surface of an outer membrane of a Gram-negative bacterium. From these data, electrostatic repulsions were expected to be more important for glycosidic surfaces (less for OH surface) than for azide surface, since the latter is less negative. The adhesion studies correlated this assumption with the decrease of the coverage rate for glycosidic surfaces. This

notwithstanding, the adhesion remained not changed with OH surface, whereas the deviation of surface free energy between OH and azide or glycosidic surfaces were similar.

Table 1. Determination of the surface free energy of the different surfaces from contact angles of water (W), formamide (FA) and diiodomethane (DI).

	Surface free energy components[a]				Total
	γ_s^{LW}	γ_s^+	γ_s^-	γ_s^{AB}	γ_s
Azide	42.25	0.50	5.19	3.23	45.48
OH	38.59	0.76	11.00	5.79	44.37
O-Glc*p*	40.89	0.83	19.11	7.94	48.83
O-Gal*p*	40.50	0.97	18.80	8.56	49.06
O-Man*p*	40.35	0.97	18.81	8.56	48.92
S-Glc*p*	40.31	1.14	16.83	8.74	49.05
S-Gal*p*	40.20	1.08	17.93	8.78	48.99
S-Man*p*	40.94	1.22	16.84	9.06	49.99
MPAO1	13.97	8.79	52.63	43.02	57.00

[a] Values in mJ/m². The surface free energy components are γ_s^{LW}: Lifshitz – van der Waals component, γ_s^+: Lewis acid component, γ_s^-: Lewis basic component, γ_s^{AB}: acid-base component.

3.6. Adhesion free energy

The thermodynamic Lifshift-van der Waals - acid-base (LW-AB) approach stipulates that the bacterial adhesion is favourable if the adhesion free energy (ΔG_{slb}^{Adh}) between surface (*s*) and bacterium (*b*) in medium (*l*) is negative, and is determined from the apolar free energy (ΔG_{slb}^{LW}) and polar free energy (ΔG_{slb}^{AB}) as:[72]

$$\Delta G_{slb}^{Adh} = \Delta G_{slb}^{LW} + \Delta G_{slb}^{AB}$$

which can be calculated from the interfacial free energy components, according to:

$$\Delta G_{slb}^{LW} = 2\left(\sqrt{\gamma_b^{LW}\gamma_l^{LW}} + \sqrt{\gamma_s^{LW}\gamma_l^{LW}} - \sqrt{\gamma_b^{LW}\gamma_s^{LW} - \gamma_l^{LW}}\right)$$

and

$$\Delta G_{slb}^{AB} = 2\left[\sqrt{\gamma_l^+}\left(\sqrt{\gamma_s^-} + \sqrt{\gamma_b^-} - \sqrt{\gamma_l^-}\right) + \sqrt{\gamma_l^-}\left(\sqrt{\gamma_s^+} + \sqrt{\gamma_b^+} - \sqrt{\gamma_l^+}\right) - \sqrt{\gamma_s^+\gamma_b^-} - \sqrt{\gamma_s^-\gamma_b^+}\right]$$

In that respect, the values of ΔG_{slb}^{Adh} between studied surfaces and *P. aeruginosa* were calculated with surface free energy components values (**Table 2**). From this approach, the interaction surface – MPAO1 was thermodynamically unfavourable with positive ΔG_{slb}^{Adh} values that implied repulsive interactions. The similar and positive ΔG_{slb}^{LW} indicated unfavorable hydrophobic interactions. The latter are the predominant interactions during the initial adhesion that occurs at long distance. Differences were noticed at the short length (hydrogen bonds) with higher values of ΔG_{slb}^{AB} after surface modifications and corroborated the assumption of greater repulsive interactions for glycosidic and OH surfaces. That being said, the model presents limits to explain the adhesion results. Indeed, adhesion differences were observed with glycosidic surfaces whereas ΔG_{slb}^{Adh} values were closed to each other. The application of this model was, to our knowledge, the first described in the literature for this type of surfaces. However, thermodynamic studies were described for the adhesion of many PAO1 strains on glass and PEG surfaces [71]. The authors determined positive ΔG_{slb}^{Adh} values (which were like our surfaces) with non-adhesive strains whereas negative values were obtained for adhesive strains. In any cases, adhesion occurred even if the adhesion were thermodynamically unfavourable. Bayoudh suggested that the LW-AB approach may explain the influence of the physicochemical properties of surfaces at the first stage of the adhesion [73]. After that, bacteria have undergone biologic changes to establish strong attachment with the surfaces.

In that respect, the LW-AB approach illustrated the adhesion trend of the low adherence of MPAO1 on surfaces. The model was, nevertheless, insufficient to undoubtedly describe the anti-bioadhesive property of glycosidic surfaces. Another phenomenon has to be taken into account, the formation of a hydration-layer with carbohydrate heads that it was suggested for similar surfaces [33]. Indeed, a structured layer of water was supposed on polar surface which created, at very short distance, repulsive forces by osmotic pressure [74]. This latter was predicted to be higher on glycosidic surface with multiple hydroxyl, rather than on OH surface.

Table 2. Values (in mJ/m²) of the adhesion free energy between MPAO1 and surfaces.

	MPAO1		
	ΔG_{slb}^{LW}	ΔG_{slb}^{AB}	ΔG_{slb}^{Adh}
Azide	3.41	7.59	11.00
OH	2.87	11.19	14.07
O-Glc*p*	3.21	15.43	18.65
O-Gal*p*	3.16	14.94	18.10
O-Man*p*	3.14	15.16	18.29
S-Glc*p*	3.13	13.62	16.75
S-Gal*p*	3.11	14.29	17.41
S-Man*p*	3.22	13.46	16.68

4. Conclusions

The ability of bacteria to develop biofilm on any surface triggers health and economic issues. Even if the process is not yet fully understood, the adhesion is the critical step which involves non-specific interactions (apolar and polar interactions) and specific interaction with adhesins or lectins. The design of materials from carbohydrates is a promising non-toxic and non-biocidal strategy to limit and to prevent the bacterial attachment.

In this respect, *O*/*S*-propargyl β-D-glucoside, *O*/*S*-propargyl β-D-galactoside or *O*/*S*-propargyl α-D-mannoside were grafted by click chemistry giving amphiphilic glass surfaces. The characterisation with water contact angle and XPS spectroscopy showed a quantitative cycloaddition reaction and a dynamic reorganization of the glycosidic layer in polar environment.

Adhesion studies of *Pseudomonas aeruginosa* MPAO1 were performed in flow chambers and a strong decrease of the adhesion was observed for glycosidic surfaces with respect to the azide surface control. However, the carbohydrate nature and the type of linkage appeared to not affect the attachment of MPAO1. Further adhesion assays with a LecA deficient mutant PAΔ*lecA* suggested that LecA was not essential for the adhesion step, nonetheless, molecular interactions may not be excluded since the complete mechanism of the adhesion remains misunderstood. The exploration of surface free energies interestingly indicated an repulsive effect between the bacterial cell wall and surfaces, expected more pronounced for glycosidic surfaces. Further thermodynamically studies have shown an unfavourable interaction of bacteria with all surfaces. The closed values of ΔG_{slb}^{LW} and ΔG_{slb}^{AB} suggested that initial adhesion was governed by the physicochemical properties in the same way for all surfaces, and the anti-

bioadhesion property of glycosidic surfaces may also result from hydration force that could reject the bacteria.

These encouraging results add more evidences that a few atomic layers of monosaccharides may minimize the bacterial attachment. Interestingly enough, the anti-bioadhesion activities were observed under static conditions that did not take in consideration the dynamism of the glycosidic layer. In fact, the glycosidic brush-layer may reduce the adhesion force enhancing the unhooking of bacteria under shear stress [75]. Finally, envisaging to extend this study by switching the carbohydrate configuration could provide information on the existence of the molecular interactions and their implications.

Conflicts of interest

There are no conflicts to declare.

Acknowledgements

The authors are grateful to the GlycoOuest (http://www.glyco-ouest.fr/) network supported by the Région Bretagne and the Région Pays de la Loire. We thank the Ministère de l'Enseignement Supérieur et de la Recherche, the CNRS for Financial supports

Supplementary Information

NMR data of glycosides, kinetic of water contact angles, XPS large spectra, microscopy images of adhered MPAO1, surface free energy components of solvents and contact angle values with water, formamide and diiodomethane.

References

[1] L. Hall-Stoodley, J.W. Costerton, P. Stoodley, Bacterial biofilms: From the natural environment to infectious diseases, Nat. Rev. Microbiol. 2 (2004) 95–108. doi:10.1038/nrmicro821.

[2] R.M. Donlan, J.W. Costerton, Biofilms, Survival Mechanisms of Clinically Relevant Microorganisms, Clin. Microbiol. Rev. 15 (2002) 167–193. doi:10.1128/CMR.15.2.167–193.2002.

[3] E. Barth, Q.M. Myrvik, W. Wagner, A.G. Gristina, In vitro and in vivo comparative colonization of Staphylococcus aureus and Staphylococcus epidermidis on orthopaedic implant materials, Biomaterials. 10 (1989) 325–328. doi:10.1016/0142-9612(89)90073-2.

[4] A.D. Pye, D.E.A. Lockhart, M.P. Dawson, C.A. Murray, A.J. Smith, A review of dental implants and infection, J. Hosp. Infect. 72 (2009) 104–110.

doi:10.1016/j.jhin.2009.02.010.

[5] C. D'Ovidio, A. Carnevale, G. Pantaleone, A. Piattelli, G. Di Bonaventura, First report of an acute purulent maxillary sinusitis caused by Pseudomonas aeruginosa secondary to dental implant placement in an immunocompetent patient, Br. Dent. J. 211 (2011) 205–207. doi:10.1038/sj.bdj.2011.723.

[6] T.W.R. Chia, R.M. Goulter, T. McMeekin, G.A. Dykes, N. Fegan, Attachment of different Salmonella serovars to materials commonly used in a poultry processing plant, Food Microbiol. 26 (2009) 853–859. doi:10.1016/j.fm.2009.05.012.

[7] E. Giaouris, E. Heir, M. Hébraud, N. Chorianopoulos, S. Langsrud, T. Møretrø, O. Habimana, M. Desvaux, S. Renier, G.J. Nychas, Attachment and biofilm formation by foodborne bacteria in meat processing environments: Causes, implications, role of bacterial interactions and control by alternative novel methods, Meat Sci. 97 (2014) 289–309. doi:10.1016/j.meatsci.2013.05.023.

[8] B. Carpentier, O. Cerf, Review - Persistence of Listeria monocytogenes in food industry equipment and premises, Int. J. Food Microbiol. 145 (2011) 1–8. doi:10.1016/j.ijfoodmicro.2011.01.005.

[9] F. Cappitelli, A. Polo, F. Villa, Biofilm Formation in Food Processing Environments is Still Poorly Understood and Controlled, Food Eng. Rev. 6 (2014) 29–42. doi:10.1007/s12393-014-9077-8.

[10] M.E. Callow, J.A. Callow, Marine biofouling: A sticky problem, Biologist. 49 (2002) 10–14. doi:10.1016/j.jacc.2008.06.042.

[11] P.Y. Qian, S.C.K. Lau, H.U. Dahms, S. Dobretsov, T. Harder, Marine biofilms as mediators of colonization by marine macroorganisms: Implications for antifouling and aquaculture, Mar. Biotechnol. 9 (2007) 399–410. doi:10.1007/s10126-007-9001-9.

[12] G. O'Toole, H.B. Kaplan, R. Kolter, Biofilm Formation as Microbial Development, Annu. Rev. Microbiol. 54 (2000) 49–79. doi:https://doi.org/10.1146/annurev.micro.54.1.49.

[13] R.M. Donlan, Biofilm Formation: A Clinically Relevant Microbiological Process, Clin. Infect. Dis. 33 (2001) 1387–1392. doi:10.1086/322972.

[14] Y.H. An, R.J. Friedman, Concise review of mechanisms of bacterial adhesion to biomaterial surfaces., J. Biomed. Mater. Res. 43 (1998) 338–348. doi:10.1002/(SICI)1097-4636(199823)43:3<338::AID-JBM16>3.0.CO;2-B.

[15] K. Hori, S. Matsumoto, Bacterial adhesion: From mechanism to control, Biochem. Eng. J. 48 (2010) 424–434. doi:10.1016/j.bej.2009.11.014.

[16] J.J.T.M. Swartjes, P.K. Sharma, T.G. Kooten, H.C. Mei, M. Mahmoudi, H.J. Busscher, E.T.J. Rochford, Current Developments in Antimicrobial Surface Coatings for Biomedical Applications, Curr. Med. Chem. 22 (2015) 2116–2129.

doi:10.2174/092986732166614091612135 5.

[17] S. Wagner, D. Hauck, M. Hoffmann, R. Sommer, I. Joachim, R. Müller, A. Imberty, A. Varrot, A. Titz, Covalent Lectin Inhibition and Application in Bacterial Biofilm Imaging, Angew. Chemie - Int. Ed. 56 (2017) 16559–16564. doi:10.1002/anie.201709368.

[18] M.L. Hawkins, F. Faÿ, K. Réhel, I. Linossier, M.L. Hawkins, F. Faÿ, K. Réhel, I. Linossier, Bacteria and diatom resistance of silicones modified with PEO-silane amphiphiles, 30 (2014) 247–258. doi:10.1080/08927014.2013.862235.

[19] F. Faÿ, M.L. Hawkins, K. Réhel, M.A. Grunlan, I. Linossier, Non-toxic, Anti-fouling Silicones with Variable PEO-silane Amphiphile Content., Green Mater. 4 (2016) 53–62. doi:10.1680/jgrma.16.00003.

[20] N. Hadjesfandiari, K. Yu, Y. Mei, J.N. Kizhakkedathu, Polymer brush-based approaches for the development of infection-resistant surfaces, J. Mater. Chem. B. 2 (2014) 4968–4978. doi:10.1039/c4tb00550c.

[21] D. Leckband, S. Sheth, A. Halperin, Grafted poly(ethylene oxide) brushes as nonfouling surface coatings, J. Biomater. Sci. Polym. Ed. 10 (1999) 1125–1147. doi:10.1163/156856299X00720.

[22] M.B. Browning, C.S. N., P.T. Luong, E.M. Cosgriff-hernandez, Determination of the in Vitro Degradation of Pegda, Jounrla Biomed. Mater. Res. Part A. 102 (2014) 4244–4251. doi:10.1002/jbm.a.35096.

[23] I. Inoshima, N. Inoshima, G. Wilke, M. Powers, K. Frank, Y. Wang, J.B. Wardenburg, PEG Hydrogel Degradation and the Role of the Surrounding Tissue Environment, J. Tssue Eng. Regen. Med. 9 (2015) 315–318. doi:10.1002/term.1688.

[24] V. Jakobi, J. Schwarze, J.A. Finlay, K.A. Nolte, S. Spöllmann, H.W. Becker, A.S. Clare, A. Rosenhahn, Amphiphilic Alginates for Marine Antifouling Applications, Biomacromolecules. 19 (2018) 402–408. doi:10.1021/acs.biomac.7b01498.

[25] S.L. McArthur, K.M. McLean, P. Kingshott, H.A.W. St John, R.C. Chatelier, H.J. Griesser, Effect of polysaccharide structure on protein adsorption, Colloids Surfaces B Biointerfaces. 17 (2000) 37–48. doi:10.1016/S0927-7765(99)00086-7.

[26] S. Bauer, M.P. Arpa-Sancet, J.A. Finlay, M.E. Callow, J.A. Callow, A. Rosenhahn, Adhesion of marine fouling organisms on hydrophilic and amphiphilic polysaccharides, Langmuir. 29 (2013) 4039–4047. doi:10.1021/la3038022.

[27] G.A. Junter, P. Thébault, L. Lebrun, Polysaccharide-based antibiofilm surfaces, Acta Biomater. 30 (2016) 13–25. doi:10.1016/j.actbio.2015.11.010.

[28] O. Rendueles, J.B. Kaplan, J.M. Ghigo, Antibiofilm polysaccharides, Environ. Microbiol. 15 (2013) 334–346. doi:10.1111/j.1462-2920.2012.02810.x.

[29] M. Hederos, P. Konradsson, B. Liedberg, Synthesis and self-assembly of galactose-terminated alkanethiols and their ability to resist proteins, Langmuir. 21 (2005) 2971–

2980. doi:10.1021/la047203b.

[30] T. Ederth, T. Ekblad, M.E. Pettitt, S.L. Conlan, C.X. Du, M.E. Callow, J.A. Callow, R. Mutton, A.S. Clare, F. D'Souza, G. Donnelly, A. Bruin, P.R. Willemsen, X.J. Su, S. Wang, Q. Zhao, M. Hederos, P. Konradsson, B. Liedberg, Resistance of galactoside-terminated alkanethiol self-assembled monolayers to marine fouling organisms, ACS Appl. Mater. Interfaces. 3 (2011) 3890–3901. doi:10.1021/am200726a.

[31] A. Myles, D. Haberlin, L. Esteban-Tejeda, M.D. Angione, M.P. Browne, M.K. Hoque, T.K. Doyle, E.M. Scanlan, P.E. Colavita, Bioinspired Aryldiazonium Carbohydrate Coatings: Reduced Adhesion of Foulants at Polymer and Stainless Steel Surfaces in a Marine Environment, ACS Sustain. Chem. Eng. 6 (2018) 1141–1151. doi:10.1021/acssuschemeng.7b03443.

[32] C. Valotteau, I.M. Banat, C.A. Mitchell, H. Lydon, R. Marchant, F. Babonneau, C.M. Pradier, N. Baccile, V. Humblot, Antibacterial properties of sophorolipid-modified gold surfaces against Gram positive and Gram negative pathogens, Colloids Surfaces B Biointerfaces. 157 (2017) 325–334. doi:10.1016/j.colsurfb.2017.05.072.

[33] C. Valotteau, N. Baccile, V. Humblot, S. Roelants, W. Soetaert, C. V. Stevens, Y.F. Dufrêne, Nanoscale antiadhesion properties of sophorolipid-coated surfaces against pathogenic bacteria, Nanoscale Horizons. (2019) 17–19. doi:10.1039/c9nh00006b.

[34] M. François-Heude, A. Méndez- Ardoy, V. Cendret, P. Lafite, R. Daniellou, C.O. Mellet, J.M. García Fernández, V. Moreau, F. Djedaïni-Pilard, Synthesis of high-mannose oligosaccharide analogues through click chemistry: True functional mimics of their natural counterparts against lectins?, Chem. - A Eur. J. 21 (2015) 1978–1991. doi:10.1002/chem.201405481.

[35] R. Périon, V. Ferrières, M.I. García-Moreno, C.O. Mellet, R. Duval, J.M. García Fernández, D. Plusquellec, 1,2,3-Triazoles and related glycoconjugates as new glycosidase inhibitors, Tetrahedron. 61 (2005) 9118–9128. doi:10.1016/j.tet.2005.07.033.

[36] K. Pachamuthu, R.R. Schmidt, Synthetic Routes to Thiooligosaccharides and Thioglycopeptides, Chem. Rev. 106 (2006) 160–187. doi:10.1021/cr040660c.

[37] Z.J. Witczak, R. Chhabra, H. Chen, X. Xie, Thiosugars II lY2 . A novel approach to thiodisaccharides The synthesis of 3-deoxy-4-thiocellobiose from levoglucosenone, Carbohydr. Res. 301 (1997) 167–175.

[38] M.A. Jacobs, A. Alwood, I. Thaipisuttikul, D. Spencer, E. Haugen, S. Ernst, O. Will, R. Kaul, C. Raymond, R. Levy, L. Chun-Rong, D. Guenthner, D. Bovee, M. V. Olson, C. Manoil, Comprehensive transposon mutant library of Pseudomonas aeruginosa, Proc. Natl. Acad. Sci. 100 (2003) 14339–14344. doi:10.1073/pnas.2036282100.

[39] A.M. Gallardo-Moreno, M.L. Navarro-Pérez, V. Vadillo-Rodríguez, J.M. Bruque, M.L.

González-Martín, Insights into bacterial contact angles: Difficulties in defining hydrophobicity and surface Gibbs energy, Colloids Surfaces B Biointerfaces. 88 (2011) 373–380. doi:10.1016/j.colsurfb.2011.07.016.

[40] H.J. Busscher, A.H. Weerkamp, H.C. van der Mei, A.W.J. van Pelt, H.P. de Jong, J. Arends, Measurement of the Surface Freen Energy of Bacterial Cell Surfaces and Its Relevance for Adhesion, Appl. Environ. Microbiol. 48 (1984) 980–983.

[41] A.L.M. Morotti, K.L. Lang, I. Carvalho, E.P. Schenkel, L.S.C. Bernardes, Semi-Synthesis of new glycosidic triazole derivatives of dihydrocucurbitacin B, Tetrahedron Lett. 56 (2015) 303–307. doi:10.1016/j.tetlet.2014.11.049.

[42] F.M. Ibatullin, S.I. Selivanov, A.G. Shavva, A General Procedure for Conversion of S-Glycosyl Isothiourea Derivatives into Thioglycosides, Thiooligosaccharides and Glycosyl Thioesters, Synthesis (Stuttg). 3 (2001) 419–422. doi:10.1055/s-2001-11443.

[43] F.M. Ibatullin, K.A. Shabalin, J. V. Jänis, A.G. Shavva, Reaction of 1,2-trans-glycosyl acetates with thiourea: A new entry to 1-thiosugars, Tetrahedron Lett. 44 (2003) 7961–7964. doi:10.1016/j.tetlet.2003.08.120.

[44] M. Lo Conte, S. Staderini, A. Marra, M. Sanchez-Navarro, B.G. Davis, A. Dondoni, Multi-molecule reaction of serum albumin can occur through thiol-yne coupling, Chem. Commun. 47 (2011) 11086. doi:10.1039/c1cc14402b.

[45] D. Giguère, M.A. Bonin, P. Cloutier, R. Patnam, C. St-Pierre, S. Sato, R. Roy, Synthesis of stable and selective inhibitors of human galectins-1 and -3, Bioorganic Med. Chem. 16 (2008) 7811–7823. doi:10.1016/j.bmc.2008.06.044.

[46] R. Lanzetta, A.M. Marzaioli, M. Parrilli, C. De Castro, E. Bedini, Conversion of yeast mannan polysaccharide in mannose oligosaccharides with a thiopropargyl linker at the pseudo-reducing end, Carbohydr. Res. 383 (2013) 43–49. doi:10.1016/j.carres.2013.10.016.

[47] L. Liang, D. Astruc, The copper(I)-catalyzed alkyne-azide cycloaddition (CuAAC) “click” reaction and its applications. An overview, Coord. Chem. Rev. 255 (2011) 2933–2945. doi:10.1016/j.ccr.2011.06.028.

[48] J.A. dos Santos, R.C.N. Reis Corrales, F.R. Pavan, C.Q.F. Leite, R.M. de Paula Dias, A.D. da Silva, Synthesis and antitubercular evaluation of new 1,2,3-triazole derivatives of carbohydrates, Mediterr. J. Chem. 1 (2012) 282–288. doi:10.13171/mjc.1.6.2012.02.05.15.

[49] S. Prakash, T.M. Long, J.C. Selby, J.S. Moore, M.A. Shannon, “ Click ” Modification of Silica Surfaces and Glass Microfluidic Channels method for covalent attachment of various polymers by and within glass microchannels suitable for CE systems . measurements , X-ray photoelectron spectroscopy , and, Anal. Chem. 79 (2007) 1661–1667. doi:10.1021/ac061824n.

[50] D. Alsteens, E. Dague, P.G. Rouxhet, A.R. Baulard, Y.F. Dufrêne, Direct measurement of hydrophobic forces on cell surfaces using AFM, Langmuir. 23 (2007) 11977–11979. doi:10.1021/la702765c.

[51] C. Barbot, O. Bouloussa, W. Szymczak, M. Plaschke, G. Buckau, J.P. Durand, J. Pieri, J.I. Kim, F. Goudard, Self-assembled monolayers of aminosilanes chemically bonded onto silicon wafers for immobilization of purified humic acids, Colloids Surfaces A Physicochem. Eng. Asp. 297 (2007) 221–239. doi:10.1016/j.colsurfa.2006.10.049.

[52] A.C. Gouget-Laemmel, J. Yang, M.A. Lodhi, A. Siriwardena, D. Aureau, R. Boukherroub, J.N. Chazalviel, F. Ozanam, S. Szunerits, Functionalization of azide-terminated silicon surfaces with glycans using click chemistry: XPS and FTIR study, J. Phys. Chem. C. 117 (2013) 368–375. doi:10.1021/jp309866d.

[53] R.K. Schulze, D.C. Boyd, J.F. Evans, W.L. Gladfelter, A variable temperature x-ray photoelectron spectroscopic study of the surface conversion of diethylaluminum azide to AlN, J. Vac. Sci. Technol. A Vacuum, Surfaces, Film. 8 (1990) 2338–2343. doi:10.1116/1.576760.

[54] E.B.M. Breidenstein, C. de la Fuente-Núñez, R.E.W. Hancock, Pseudomonas aeruginosa: All roads lead to resistance, Trends Microbiol. 19 (2011) 419–426. doi:10.1016/j.tim.2011.04.005.

[55] J.B. Lyczak, C.L. Cannon, G.B. Pier, Establishment of Pseudomonas aeruginosa infection: Lessons from a versatile opportunist, Microbes Infect. 2 (2000) 1051–1060. doi:10.1016/S1286-4579(00)01259-4.

[56] M.D. Obritsch, D.N. Fish, R. MacLaren, R. Jung, Nosocomial infections due to multidrug-resistant Pseudomonas aeruginosa: Epidemiology and treatment options, Pharmacotherapy. 25 (2005) 1353–1364. doi:10.1592/phco.2005.25.10.1353.

[57] M. Hermansson, The DLVO theory in microbial adhesion, Colloids Surfaces B Biointerfaces. 14 (1999) 105–119. doi:10.1016/S0927-7765(99)00029-6.

[58] A. Zita, M. Hermansson, Effects of bacterial cell surface structures and hydrophobicity on attachment to activated sludge flocs, Appl. Environ. Microbiol. 63 (1997) 1168–1170. doi:10.1023/A:1012883811652.

[59] R. Bos, H.C. Van Der Mei, H.J. Busscher, Physico-chemistry of initial microbial adhesive interactions - Its mechanisms and methods for study, FEMS Microbiol. Rev. 23 (1999) 179–229. doi:10.1016/S0168-6445(99)00004-2.

[60] S. Kesel, A. Mader, P.H. Seeberger, O. Lieleg, M. Opitz, Carbohydrate coating reduces adhesion of biofilm-forming Bacillus subtilis to gold surfaces, Appl. Environ. Microbiol. 80 (2014) 5911–5917. doi:10.1128/AEM.01600-14.

[61] T.K. Lindhorst, Small Molecule Ligands for Bacterial Lectins : Letters of an

Antiadhesive Glycopolymer Code, in: L. Hartmann, C.R. Becer (Eds.), Glycopolymer Code Synth. Glycopolymers Their Appl., RSC Publishing, 2015: pp. 10–20.

[62] T. Weber, V. Chandrasekaran, I. Stamer, M.B. Thygesen, A. Terfort, T.K. Lindhorst, Switching of Bacterial Adhesion to a Glycosylated Surface by Reversible Reorientation of the Carbohydrate Ligand., Angew. Chemie - Int. Ed. 53 (2014) 14583–14586. doi:10.1002/anie.201409808.

[63] A. Imberty, M. Wimmerová, E.P. Mitchell, N. Gilboa-Garber, Structures of the lectins from Pseudomonas aeruginosa: Insights into the molecular basis for host glycan recognition, Microbes Infect. 6 (2004) 221–228. doi:10.1016/j.micinf.2003.10.016.

[64] G. Cioci, E.P. Mitchell, C. Gautier, M. Wimmerová, D. Sudakevitz, S. Pérez, N. Gilboa-Garber, A. Imberty, Structural basis of calcium and galactose recognition by the lectin PA-IL of Pseudomonas aeruginosa, FEBS Lett. 555 (2003) 297–301. doi:10.1016/S0014-5793(03)01249-3.

[65] N. Garber, U. Guempel, A. Belz, N. Gilboa-Garber, R.J. Doyle, On the specificity of the d-galactose-binding lectin (PA-I) of Pseudomonas aeruginosa and its strong binding to hydrophobic derivatives of d-galactose and thiogalactose, Biochim. Biophys. Acta. 1116 (1992) 331–333. doi:10.1016/0304-4165(92)90048-Y.

[66] S.P. Diggle, R.E. Stacey, C. Dodd, M. Cámara, P. Williams, K. Winzer, The galactophilic lectin, LecA, contributes to biofilm development in Pseudomonas aeruginosa, Environ. Microbiol. 8 (2006) 1095–1104. doi:10.1111/j.1462-2920.2006.001001.x.

[67] C.J. van Oss, M.K. Chaudhury, R.J. Good, Monopolar Surfaces, Adv. Colloid Interface Sci. 28 (1987) 35–64. doi:10.23736/S0375-9393.17.11967-X.

[68] C.J. van Oss, R.J. Good, M.K. Chaudhury, The Role of van der Waals Forces and Hydrogen Bonds in " Hydrophobic Interactions " between Biopolymers and Low Energy Surfaces, J. Colloid Interface Sci. 111 (1986) 378–390.

[69] R.J. Good, Contact angle, wetting, and adhesion: a critical review, J. Adhes. Sci. Technol. 6 (1992) 1269–1302.

[70] R.S. Drago, Quantitative evaluation and prediction of donor-acceptor interactions, Coord. Interact. (2006) 73–139. doi:10.1007/bfb0036784.

[71] A. Roosjen, H.J. Busscher, W. Norde, H.C. Van der Mei, Bacterial factors influencing adhesion of Pseudomonas aeruginosa strains to a poly(ethylene oxide) brush, Microbiology. 152 (2006) 2673–2682. doi:10.1099/mic.0.29005-0.

[72] P.K. Sharma, K. Hanumantha Rao, Analysis of different approaches for evaluation of surface energy of microbial cells by contact angle goniometry, Adv. Colloid Interface Sci. 98 (2002) 341–463. doi:10.1016/S0001-8686(02)00004-0.

[73] S. Bayoudh, A. Othmane, F. Bettaieb, A. Bakhrouf, H. Ben Ouada, L. Ponsonnet,

Quantification of the adhesion free energy between bacteria and hydrophobic and hydrophilic substrata, Mater. Sci. Eng. C. 26 (2006) 300–305. doi:10.1016/j.msec.2005.10.045.

[74] V.A. Parsegian, T. Zemb, Hydration forces: Observations, explanations, expectations, questions, Curr. Opin. Colloid Interface Sci. 16 (2011) 618–624. doi:10.1016/j.cocis.2011.06.010.

[75] M.R. Nejadnik, H.C. van der Mei, W. Norde, H.J. Busscher, Bacterial adhesion and growth on a polymer brush-coating, Biomaterials. 29 (2008) 4117–4121. doi:10.1016/j.biomaterials.2008.07.014.

[76] N. Pietrzik, C. Schips, T. Ziegler, Efficient synthesis of glycosylated asparaginic acid building blocks via click chemistry, Synthesis (Stuttg). (2008) 0519–0526. doi:10.1055/s-2008-1032150.

Supplementary Information

Pseudomonas aeruginosa resistance of monosaccharide-Functionalized glass surfaces

Mathieu Scalabrini [a], Jonathan Hamon [c], Isabelle Linossier [a], Vincent Ferrières [b] and Karine Réhel [a]

[a]Univ Bretagne-Sud, EA 3884, LBCM, IUEM, F-56100 Lorient, France.

[b]Univ Rennes, école Nationale Supérieure de Chimie de Rennes, CNRS, ISCR – UMR6226, F-35000 Rennes, France.

[c]Institut des Matériaux Jean Rouxel (IMN), Université de Nantes, CNRS UMR6502, Institut des Matériaux Jean Rouxel, 2 rue de la Houssinière, BP32229, Nantes Cedex 3 44322, France

NMR data of glycosides 1-4

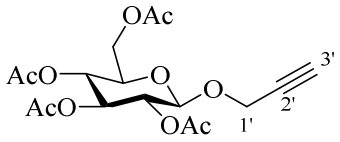

Propargyl 2,3,4,6-tetra-*O*-acetyl-1-*O*-β-D-glucopyranoside (1a) [1]

Title compound was synthesized from Acetyl 2,3,4,6-tetra-*O*-acetyl-1-*O*-β-D-glucopyranoside (7.77 mmol, 3.03 g) and afforded product (7.04 mmol, 2,72 g, 91%) as yellow solid. R_f = 0.42 in cyclohexane/EtOAc (5:5).

^{1}H NMR (400 MHz, $CDCl_3$) δ 5.24 (t, $J_{3,2}$ = 9.6 Hz, 1H, H3), 5.10 (dd, $J_{4,5}$ = 10.0 Hz, $J_{4,3}$ = 9.6 Hz, 1H, H4), 5.02 (dd, $J_{2,3}$ = 9.6 Hz, $J_{2,1}$ = 8.0 Hz, 1H, H2), 4.78 (d, $J_{1,2}$ = 8.0 Hz, 1H, H1), 4.37 (d, $J_{1',3'}$ = 2.4 Hz, 2H, H1'), 4.28 (dd, $J_{6a,6b}$ = 12.4 Hz, $J_{6a,5}$ = 4.6 Hz, 1H, H6a), 4.15 (dd, $J_{6b,6a}$ = 12.4 Hz, $J_{6b,5}$ = 2.4 Hz, 1H, H6b), 3.73 (ddd, $J_{5,4}$ = 10.0 Hz, $J_{5,6a}$ = 4.6 Hz, $J_{5,6b}$ = 2.4 Hz, 1H, H5), 2.47 (t, $J_{3',1'}$ = 2.4 Hz, 1H, H3'), 2.09, 2.06, 2.03, 2.01 (s, 12H, 4 x CH3,OAc).

^{13}C NMR (101 MHz, $CDCl_3$) δ 170.8, 170.4, 169.6, 169.5 (4 x C=O), 98.3 (C-1), 78.2 (C-2'), 75.6 (C-3'), 72.9 (C-2), 72.1 (C-3), 71.1 (C-4), 68.4 (C-5), 61.9 (C-6), 56.1 (C-1'), 20.9, 20.8, 20.8, 20.7 (4 x *C*H_3CO).

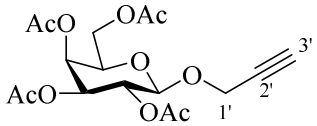

Propargyl 2,3,4,6-tetra-*O*-acetyl-1-*O*-β-D-galactopyranoside (1b) [1]

Title compound was synthesized from Acetyl 2,3,4,6-tetra-*O*-acetyl-1-*O*-β-D-galactopyranoside (7.69 mmol, 3 g) and afforded product (7.67 mmol, 2,96 g, 98%) as yellow-orange solid. R_f = 0.42 in cyclohexane/EtOAc (5:5).

^{1}H NMR (400 MHz, $CDCl_3$) δ 5.40 (dd, $J_{4,3}$ = 3.4 Hz, $J_{4,5}$ = 1.2 Hz, 1H, H4), 5.22 (dd, $J_{2,3}$ = 10.5 Hz, $J_{2,1}$ = 8.0 Hz, 1H, H2), 5.06 (dd, $J_{3,2}$ = 10.5 Hz, $J_{3,4}$ = 3.4 Hz, 1H, H3), 4.73 (d, $J_{1,2}$ = 8.0 Hz, 1H, H1), 4.38 (d, $J_{1',3'}$ = 2.4 Hz, 2H, H1'), 4.25 – 4.08 (m, 2H, H6), 3.93 (dt, $J_{5,6}$ = 6.7 Hz, $J_{5,6}$ = 1.2 Hz, 1H, H5), 2.46 (t, $J_{3',1'}$ = 2.4 Hz, 1H, H3'), 2.15, 2.07, 2.05, 2.0 (s, 12H, 4 x CH3,OAc).

^{13}C NMR (101 MHz, $CDCl_3$) δ 170.5, 170.3, 169.8, 169.7 (4 x C=O), 98.8 (C-1), 78.3 (C-2'), 75.5 (C-3'), 71.1 (C-2), 71.0 (C-3), 68.6 (C-4), 67.1 (C-5), 61.3 (C-6), 56.0 (C-1'), 20.9, 20.8, 20.8, 20.7 (4 x *C*H_3CO).

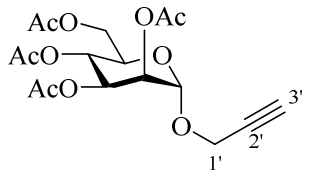

Propargyl 2,3,4,6-tetra-*O*-acetyl-1-*O*-α-D-mannopyranoside (1c) [1]

Title compound was synthesized from Acetyl 2,3,4,6-tetra-*O*-acetyl-1-*O*-α/β-D-mannopyranoside (7.77 mmol, 3.03 g) and afforded product (7.67 mmol, 2,96 g, 99%) as yellow oil. R_f = 0.43 in cyclohexane/EtOAc (5:5).

^{1}H NMR (400 MHz, $CDCl_3$) δ 5.36 – 5.29 (m, 2H, H3, H4), 5.27 (dd, $J_{2,3}$ = 3.2 Hz, $J_{2,1}$ = 1.7 Hz, 1H, H2), 5.02 (d, $J_{1,2}$ = 1.7 Hz, 1H, H1), 4.31 – 4.25 (m, 3H, H-6a, H1'), 4.10 (dd, $J_{6b,6a}$ = 12.3 Hz, $J_{6b,5}$ = 2.5 Hz, 1H, H6b), 4.01 (ddd, $J_{5,4}$ = 9.3 Hz, $J_{5,6a}$ = 5.2 Hz, $J_{5,6b}$ = 2.5 Hz, 1H, H5), 2.47 (t, $J_{3',1'}$ = 2.4 Hz, 1H, H3'), 2.16, 2.10, 2.03, 1.98 (s, 12H, 4 x CH_3,OAc).

^{13}C NMR (101 MHz, $CDCl_3$) δ 170.6, 169.9, 169.8, 169.7 (4 x C=O), 96.2 (C-1), 77.9 (C-2'), 75.6 (C-3'), 69.3 (C-2), 69.0 (C-3), 68.9 (C-4), 66.0 (C-5), 62.3 (C-6), 55.0 (C-1'), 20.9, 20.7, 20.7, 20.7 (s, 12H, 4 x *C*H_3OAc).

Propargyl 1-*O*-β-D-glucopyranoside (2a) [1]

Title compound was synthesized from 1a (2.59 mmol, 1 g) and afforded product (2.11 mmol, 460 mg, 81%) as white powder. R_f = 0.21 in DCM/MeOH (9:1).

^{1}H NMR (400 MHz, D_2O) δ 4.65 (d, $J_{1,2}$ = 8.0 Hz, 1H, H1), 4.54 – 4.42 (m, 2H, H1'), 3.93 (dd, $J_{6a,6b}$ = 12.4 Hz, $J_{6a,5}$ = 2.2 Hz, 1H), 3.73 (dd, $J_{6b,6a}$ = 12.4 Hz, $J_{6b,5}$ = 5.8 Hz, 1H, H6b), 3.55 – 3.35 (m, 3H, H3, H4, H5), 3.30 (dd, $J_{2,3}$ = 9.3 Hz, $J_{2,1}$ = 8.0 Hz, 1H, H2), 2.93 (t, $J_{3',1'}$ = 2.4 Hz, 1H).

^{13}C NMR (101 MHz, D_2O) δ 100.5 (C-1), 78.8 (C-2'), 76.3 (C-3'), 76.0 (C-3), 75.7 (C-5), 72.9 (C-2), 69.5 (C-4), 60.6 (C-6), 56.5 (C-1').

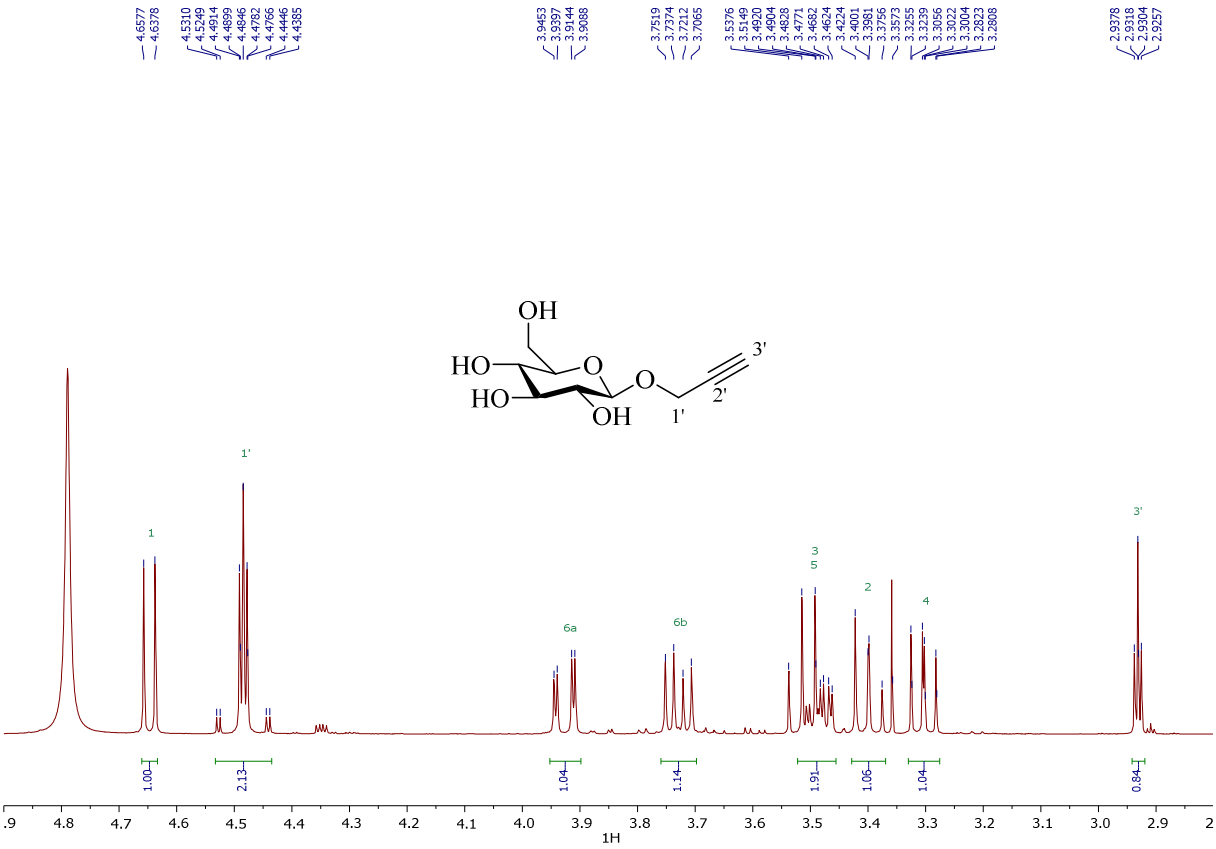

Propargyl 1-*O*-β-D-galactopyranoside (2b) [1]

Title compound was synthesized from 1b (2.59 mmol, 1 g) and afforded product (1.41 mmol, 308 mg, 55%) as white powder. R_f = 0.21 in DCM/MeOH (9:1).

^{1}H NMR (400 MHz, D_2O) δ 4.58 (d, $J_{1,2}$ = 7.9 Hz, 1H, H1), 4.54 – 4.42 (m, 2H, H1'), 3.94 (dd, $J_{4,3}$ = 3.4 Hz, $J_{4,5}$ = 1.0 Hz, 1H, H4), 3.83 – 3.70 (m, 3H, H6, H5), 3.67 (dd, $J_{3,2}$ = 9.9, $J_{3,4}$ = 3.4 Hz, 1H, H3), 3.54 (dd, $J_{2,3}$ = 9.9 Hz, $J_{2,1}$ = 7.9 Hz, 1H, H2), 2.92 (t, $J_{3',1'}$ = 2.4 Hz, 1H, H3').

^{13}C NMR (101 MHz, D_2O) δ 101.1 (C-1), 78.8 (C-2'), 76.2 (C-3'), 75.2 (C-5), 72.7 (C-3), 70.5 (C-2), 68.6 (C-4), 60.9 (C-6), 56.5 (C-1').

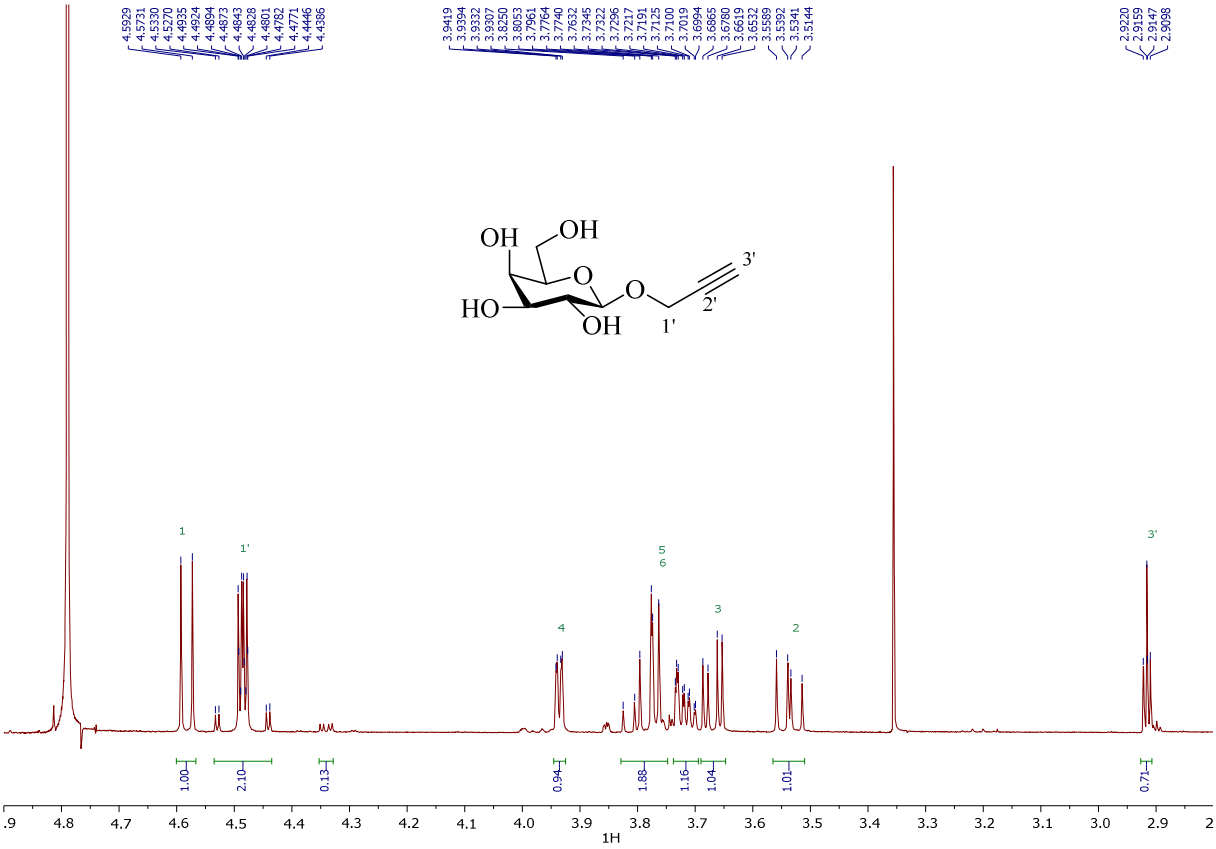

Propargyl 1-*O*-β-D-mannopyranoside (2c) [1]

Title compound was synthesized from 1c (2.59 mmol, 1 g) and afforded product (1.92 mmol, 420 mg, 74%) as white powder. R_f = 0.22 in DCM/MeOH (9:1).

^{1}H NMR (400 MHz, D_2O) δ 5.04 (d, $J_{1,2}$ = 1.8 Hz, 1H, H1), 4.41 – 4.27 (m, 2H, H1'), 3.96 (dd, $J_{2,3}$ = 3.4 Hz, $J_{2,1}$ = 1.8 Hz, 1H, H2), 3.89 (dd, $J_{6a,6b}$ = 12.2 Hz, $J_{6a,5}$ = 1.7 Hz, 1H, H-6a), 3.83 – 3.74 (m, 2H, H5, H6b), 3.71 – 3.64 (m, 2H, H3, H4), 2.92 (t, $J_{3',1'}$ = 2.4 Hz, 1H, H3').

^{13}C NMR (101 MHz, D_2O) δ 98.7 (C-1), 78.7 (C-2'), 76.1 (C-3'), 73.1 (C-5), 70.4 (C-3), 69.9 (C-2), 66.5 (C-4), 60.7 (C-6), 54.5 (C-1').

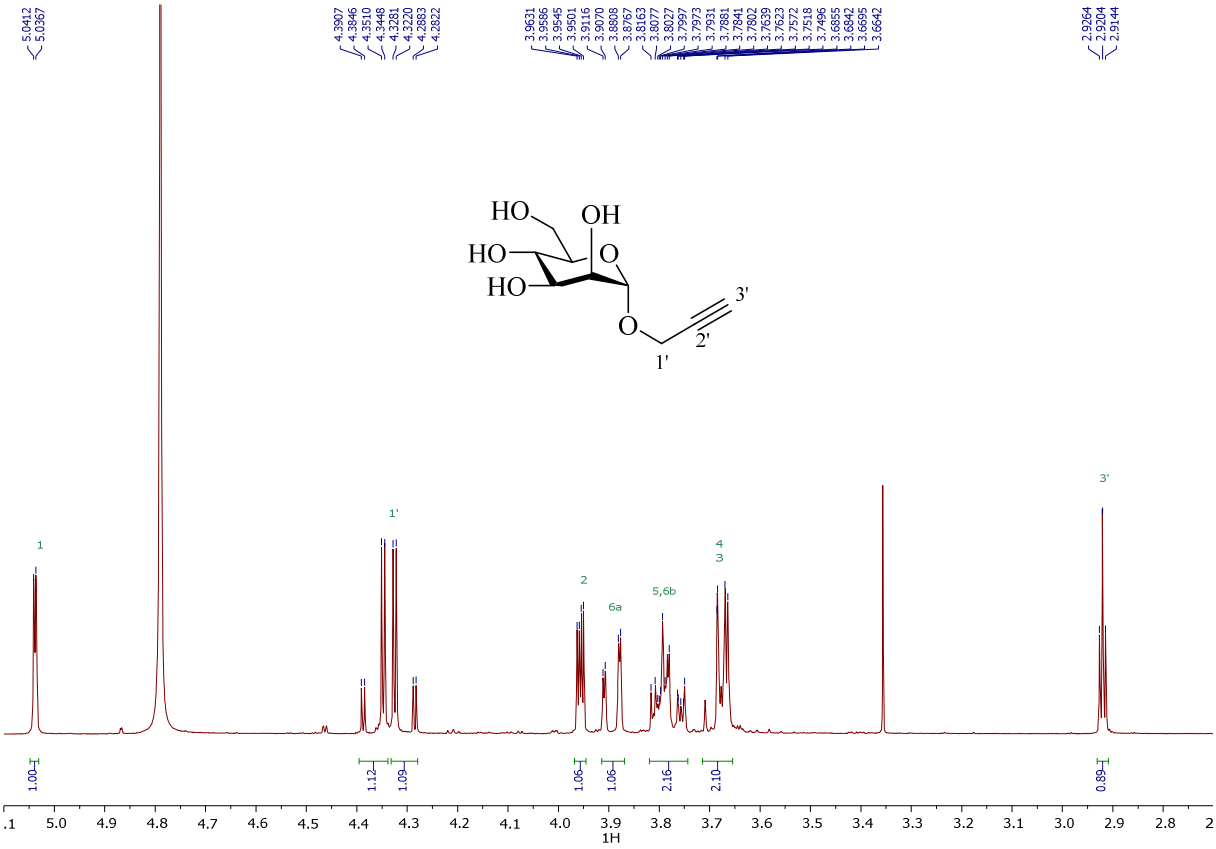

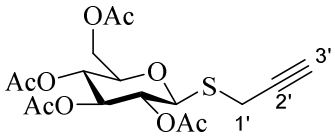

Propargyl 2,3,4,6-tetra-*O*-acetyl-1-thio-β-D-glucopyranoside (3a) [2]

Title compound was synthesized from Acetyl 2,3,4,6-tetra-*O*-acetyl-1-*O*-β-D-glucopyranoside (12.81 mmol, 5 g) and afforded product (6.91 mmol, 2,78 g, 54%) as yellow oil. R_f = 0.28 in cyclohexane/EtOAc (7:3).

^{1}H NMR (400 MHz, $CDCl_3$) δ 5.22 (t, $J_{3,4}$ = 9.4 Hz, 1H, H3), 5.03 (m, 2H, H2, H4), 4.73 (d, $J_{1,2}$ = 10.1 Hz, 1H, H1), 4.21 (dd, $J_{6a,6b}$ = 12.4 Hz, $J_{6a,5}$ = 4.9 Hz, 1H, H6a), 4.10 (dd, $J_{6b,6a}$ = 12.4 Hz, $J_{6b,5}$ = 2.3 Hz, 1H, H6b), 3.70 (ddd, $J_{5,4}$ = 10.1 Hz, $J_{5,6a}$ = 4.9 Hz, $J_{5,6b}$ = 2.3 Hz, 1H, H5), 3.51 (dd, $J_{1'a,1'b}$ = 16.5 Hz, $J_{1'a,3'}$ = 2.6 Hz, 1H, H1'a), 3.25 (dd, $J_{1'b,1'a}$ = 16.5 Hz, $J_{1'b,3'}$ = 2.6 Hz, 1H, H1'b), 2.24 (t, $J_{3',1'}$ = 2.6 Hz, 1H, H3'), 2.03, 2.01, 1.98, 1.96 (s, 12H, 4 x CH_3,OAc).

^{13}C NMR (101 MHz, $CDCl_3$) δ 170.6, 170.1, 169.4, 169.3 (4 x C=O), 82.0 (C-1), 78.7 (C-2'), 75.9 (C-5), 73.7 (C-3), 72.0 (C-3'), 69.7 (C-2), 68.2 (C-4), 61.9 (C-6), 20.7, 20.6, 20.5, 20.5 (4 x *C*H_3OAc), 17.5 (C-1').

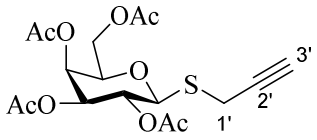

Propargyl 2,3,4,6-*O*-acetyl-1-thio-β-D-galactopyranoside (3b) [2]

Title compound was synthesized from Acetyl 2,3,4,6-tetra-*O*-acetyl-1-*O*-β-D-galactopyranoside (12.81 mmol, 5 g) and afforded product (7.04 mmol, 2.83 g, 55%) as orange oil. R_f = 0.28 in cyclohexane/EtOAc (7:3).

^{1}H NMR (400 MHz, $CDCl_3$) δ 5.43 (dd, $J_{4,3}$ = 3.5 Hz, $J_{4,5}$ = 1.1 Hz, 1H, H-4), 5.32 – 5.20 (m, 1H, H-2), 5.08 (dd, $J_{3,2}$ = 9.9 Hz, $J_{H3\text{-}H4}$ = 3.5 Hz, 1H, H-3), 4.73 (d, $J_{1,2}$ = 10.0 Hz, 1H, H-1), 4.21 – 4.06 (m, 2H, H-6a, H-6b), 3.96 (dt, $J_{5,6}$ = 6.6, $J_{5,4}$ = 1.1 Hz, 1H, H-5), 3.56 (dd, $J_{1'a,1'b}$ = 16.5 Hz, $J_{1'a,3'}$ = 2.6 Hz, 1H, H-1'a), 3.29 (dd, $J_{1'b,1'a}$ = 16.5 Hz, $J_{1'b,3'}$ = 2.6 Hz, 1H, H-1'a), 2.26 (t, $J_{3',1'}$ = 2.6 Hz, 1H, H-3'), 2.14, 2.06, 2.03, 1.97 (s, 12H, CH_3,OAc).

^{13}C NMR (101 MHz, $CDCl_3$) δ 170.6, 170.1, 169.4, 169.3 (4 x C=O), 82.0 (C-1), 78.7 (C-2'), 75.9 (C-5), 73.7 (C-3), 72.0 (C-3'), 69.7 (C-2), 68.2 (C-4), 61.9 (C-6), 20.7, 20.6, 20.6, 20.5 (4 x *C*H_3 OAc), 17.5 (C-1').

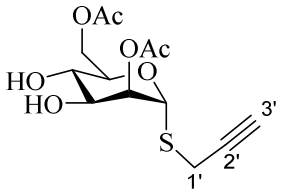

Propargyl 2,3,4,6-*O*-acetyl-1-thio-β-D-mannopyranoside (3c) [2]

Title compound was synthesized from Acetyl 2,3,4,6-tetra-*O*-acetyl-1-*O*-α/β-D-galactopyranoside (402,41 mmol, 10 g) and afforded product (2.39 mmol, 964 mg, 9%) as white powder. R_f = 0.25 in cyclohexane/EtOAc (7:3).

^{1}H NMR (400 MHz, $CDCl_3$) δ 5.50 (d, $J_{1,2}$ = 1.5 Hz, 1H, H1), 5.39 (dd, $J_{2,3}$ = 3.4 Hz, $J_{2,1}$ = 1.5 Hz, 1H, H2), 5.34 (m, 1H, H4), 5.24 (dd, $J_{3,4}$ = 10.0 Hz, $J_{3,2}$ = 3.4 Hz, 1H, H3), 4.38 – 4.31 (m, 2H, H5, H6a), 4.14 – 4.08 (m, 1H, H6b), 3.41 (dd, $J_{1'a,1'b}$ = 16.8 Hz, $J_{1'a,3'}$ = 2.6 Hz, 1H, H1'a), 3.24 (dd, $J_{1'b,1'a}$ = 16.8 Hz, $J_{1'b,3'}$ = 2.6 Hz, 1H, H1'b), 2.27 (t, $J_{3',1'}$ = 2.6 Hz, 1H, H3').

^{13}C NMR (101 MHz, $CDCl_3$) δ 170.6, 169.8, 169.8, 169.6 (4 x C=O), 81.5 (C-1), 78.4 (C-2'), 72.1 (C-3'), 70.4 (C-2), 69.6 (C-3), 69.4 (C-5), 66.2 (C-4), 62.3 (C-6), 20.9, 20.7, 20.7, 20.6 (4 x *C*H_3 O Ac), 18.1 (C-1').

Propargyl 1-thio-β-D-glucopyranoside (4a) [3]

Title compound was synthesized from 3a (2.48 mmol, 1 g) and afforded product (1.56 mmol, 364 mg, 63%) as yellow powder. R_f = 0.18 in DCM/MeOH (9:1).

^{1}H NMR (400 MHz, D_2O) δ 4.74 (d, $J_{1,2}$ = 9.9 Hz, 1H, H1), 3.92 (dd, $J_{6a,6b}$ = 12.5 Hz, $J_{6a,5}$ = 2.2 Hz, 1H, H6a), 3.72 (dd, $J_{6b,6a}$ = 12.5 Hz, $J_{6b,5}$ = 5.6 Hz, 1H, H6b), 3.63 (dd, $J_{1'a,1'b}$ = 17.0 Hz, $J_{1'a,3'}$ = 2.6 Hz, 1H, H1'a), 3.55 – 3.49 (m, 2H, H4, H5), 3.47 (dd, $J_{1'b,1'a}$ = 17.0 Hz, $J_{1'b,3'}$ = 2.6 Hz, 1H, H1'b), 3.45 – 3.40 (m, 2H, H2, H3), 2.67 (t, $J_{3',1'}$ = 2.6 Hz, 1H, H3').

^{13}C NMR (101 MHz, D_2O) δ 84.1 (C-1), 80.3 (C-2'), 79.9 (C-5), 77.2 (C-4), 72.2 (C-3'), 71.9 (C-2), 69.4 (C-3), 60.8 (C-6), 16.9 (C-1').

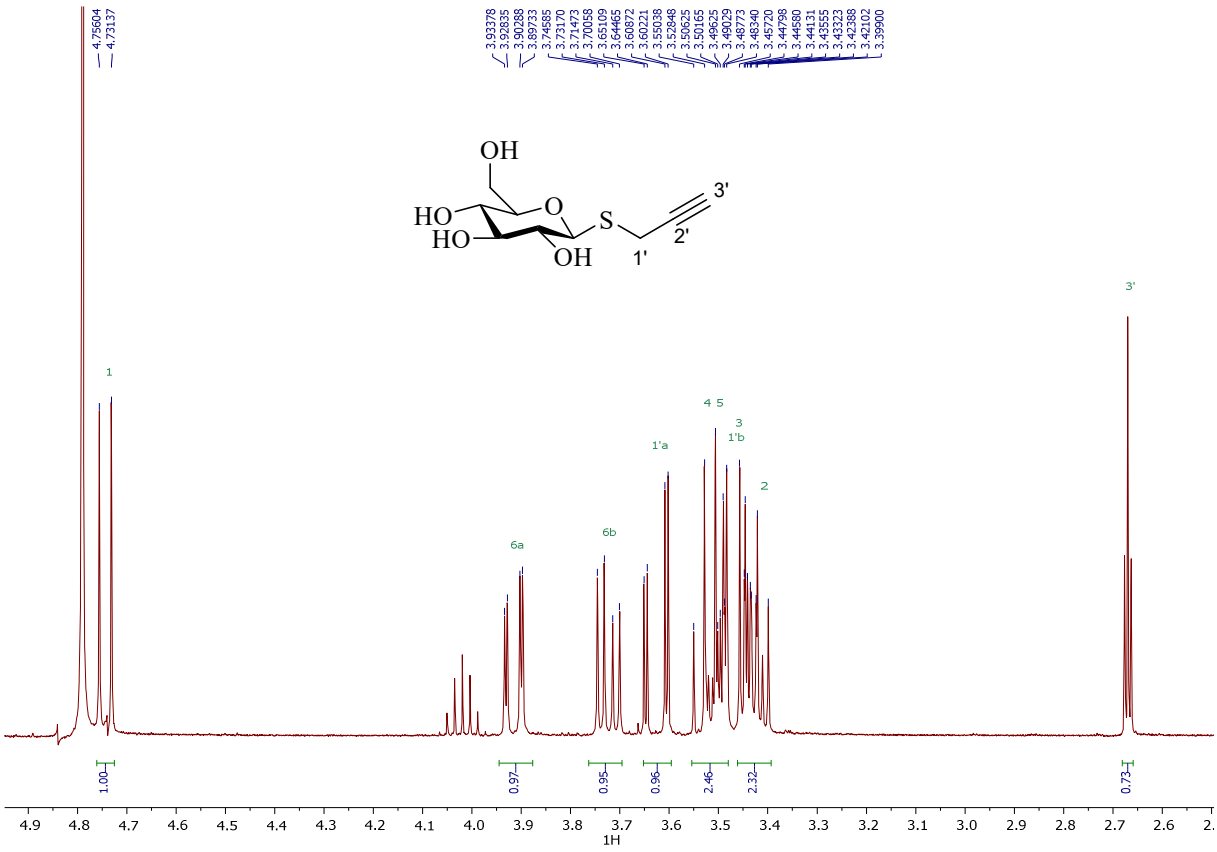

Propargyl 1-thio-β-D-galactopyranoside (4b) [4]

Title compound was synthesized from 3b (0.99 mmol, 400 mg) and afforded product (0.64 mmol, 149 mg, 81%) as white powder. R_f = 0.18 in DCM/MeOH (9:1).

^{1}H NMR (400 MHz, CD_3OD) δ 4.52 (d, $J_{1,2}$ = 9.7 Hz, 1H, H1), 3.90 (dd, $J_{4,3}$ = 3.3 Hz, $J_{4,5}$ = 1.1 Hz, 1H, H4), 3.76 (dd, $J_{6a,6b}$ = 11.5 Hz, $J_{6a,5}$ = 6.9 Hz, 1H, H6a), 3.69 (dd, $J_{6b,6a}$ = 11.5 Hz, $J_{6b,5}$ = 5.2 Hz, 1H, H6b), 3.63 – 3.57 (m, 2H, H2, H1'a), 3.54 (ddd, $J_{5,6a}$ = 6.9 Hz, $J_{5,6b}$ = 5.2 Hz,

$J_{5,4}$ = 1.1 Hz, 1H, H-5), 3.48 (dd, $J_{3,2}$ = 9.2 Hz, $J_{3,4}$ = 3.3 Hz, 1H, H-3), 3.41 (dd, $J_{1'b,1'a}$ = 16.4 Hz, $J_{1'b,3'}$ = 2.7 Hz, 1H, H-1'b), 2.57 (t, $J_{3',1'}$ = 2.7 Hz, 1H, H-3').

^{13}C NMR (101 MHz, CD_3OD) δ 86.1 (C-1), 80.8 (C-2'), 80.7 (C-5), 76.2 (C-3), 72.3 (C-3'), 71.2 (C-2), 70.5 (C-4), 62.6 (C-6), 17.5 (C-1').

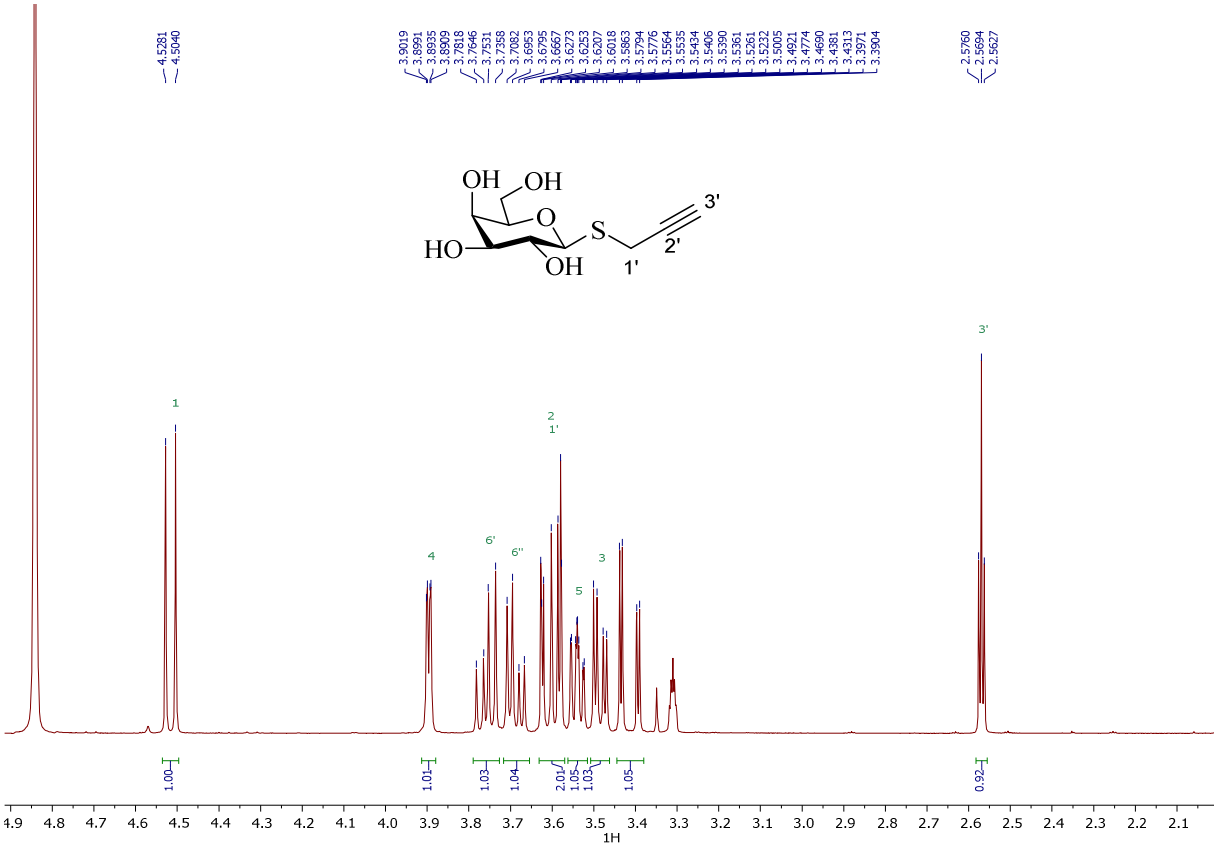

Propargyl 1-thio-α-D-mannopyranoside (4c) [5]

Title compound was synthesized from 3b (1,24 mmol, 500 mg) and afforded product (1.02 mmol, 240 mg, 74%) as colorless oil. R_f = 0.18 in DCM/MeOH (9:1).

^{1}H NMR (400 MHz, D_2O) δ 5.51 (d, $J_{1,2}$ = 1.4 Hz, 1H, H1), 4.09 (dd, $J_{2,3}$ = 3.3 Hz, $J_{2,1}$ = 1.4 Hz, 1H, H2), 4.00 – 3.94 (m, 1H, H5), 3.90 (dd, $J_{6a,6b}$ = 12.3 Hz, $J_{6a,5}$ = 2.3 Hz, 1H, H6a), 3.82 – 3.69 (m, 3H, H3, H4, H6b), 3.48 (dd, $J_{1'a,1'b}$ = 17.1 Hz, $J_{1'a,3'}$ = 2.6 Hz, 1H, H1'a), 3.36 (dd, $J_{1'b,1'a}$ = 17.0 Hz, $J_{H1'b\text{-}H3'}$ = 2.6 Hz, 1H, H1'b), 2.69 (t, $J_{3',1'}$ = 2.6 Hz, 1H, H3').

^{13}C NMR (101 MHz, D_2O) δ 83.7 (C-1), 80.0 (C-2'), 73.4 (C-5), 72.2 (C-3'), 71.3 (C-2), 71.2 (C-3), 66.9 (C-4), 60.7 (C-6), 17.4 (C-1').

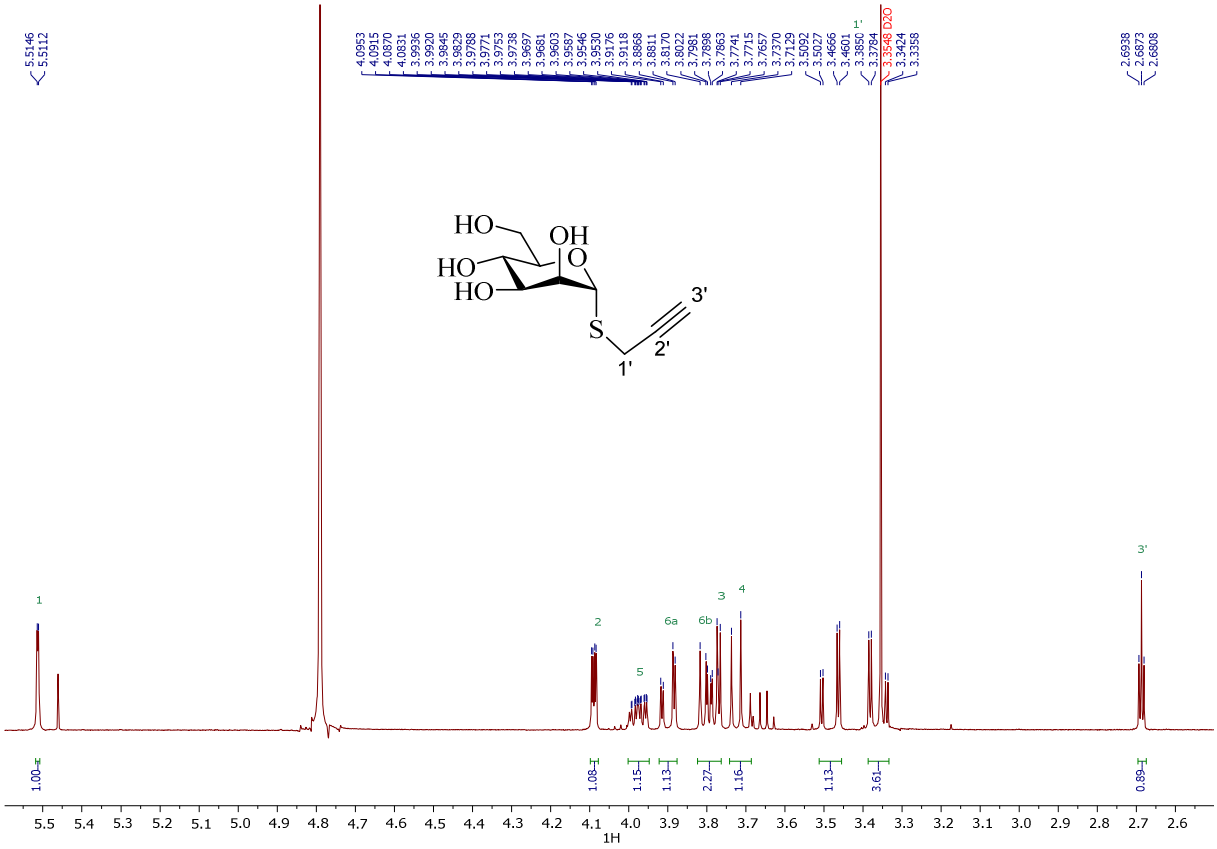
HO
OH
HO
O
HO
S
3'
2'
1'
1
2
5
6a
6b
3
4
3'
1.00
1.08
1.15
1.13
2.27
1.16
1.13
3.61
0.89
1H

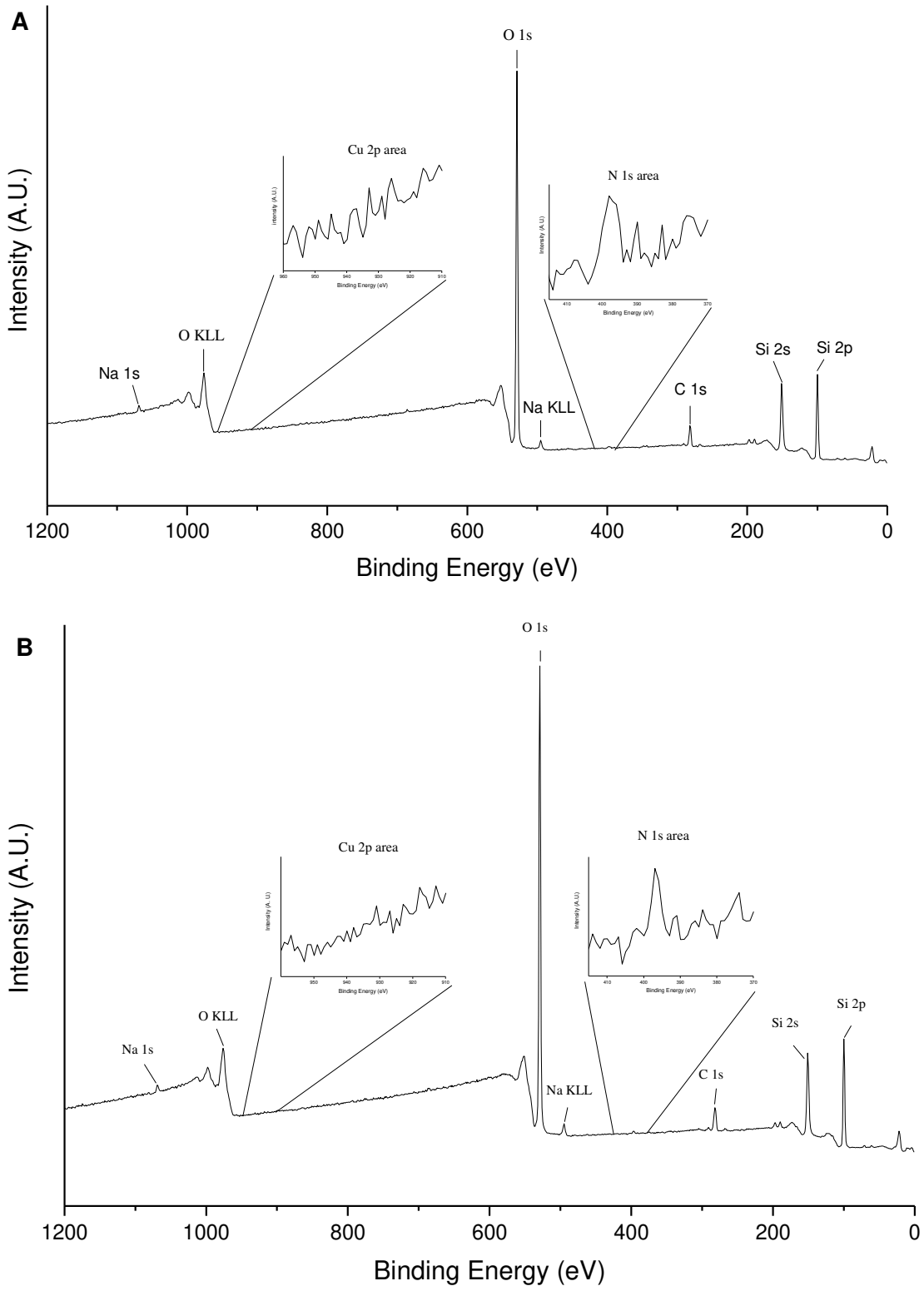

Figure S1. XPS large spectrum of (A) azide and (B) *O*-Glc*p* surface with the attribution of the principal signals. (All functionalized surfaces have presented similar spectrum, without signal for Cu 2p)

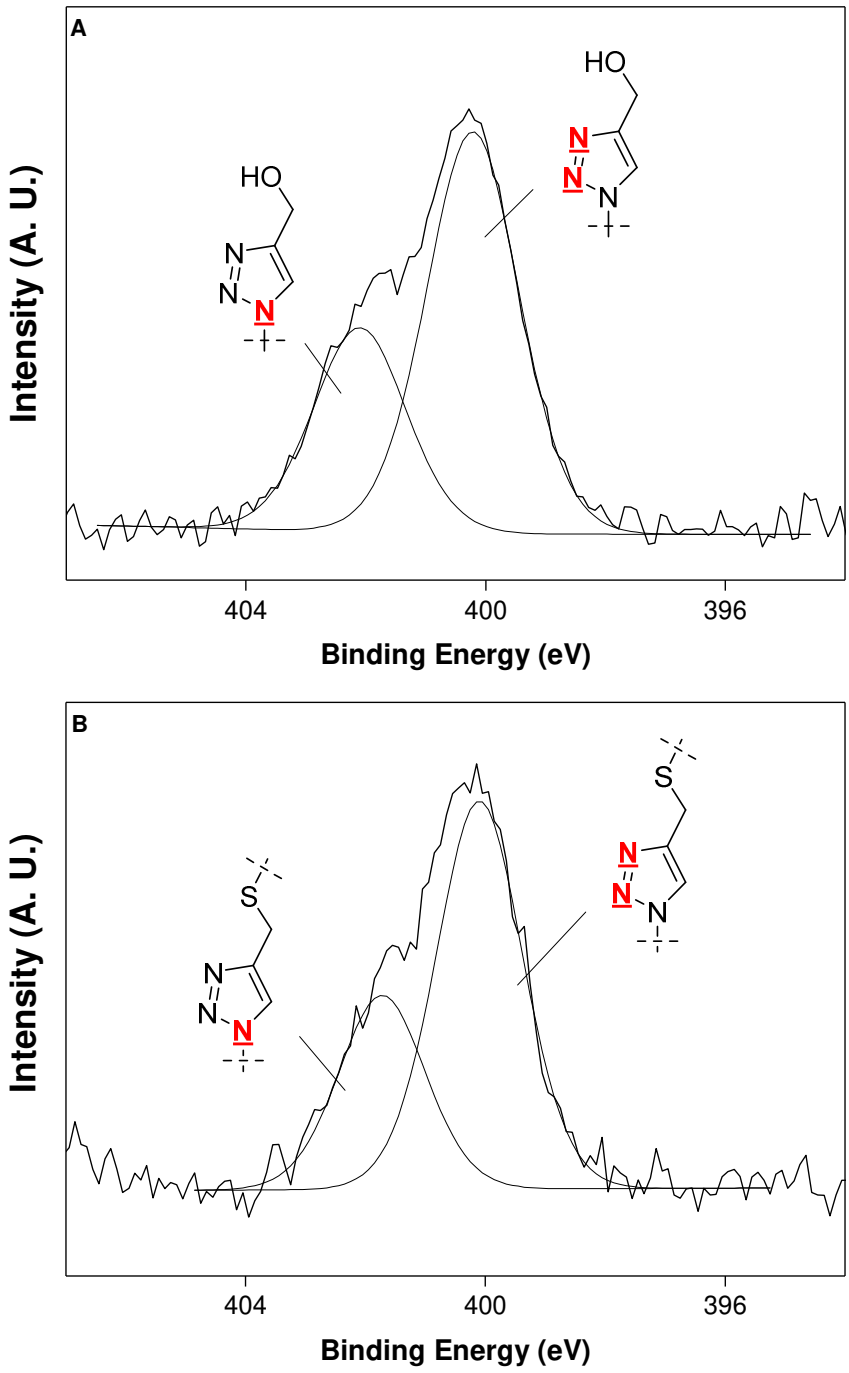

Figure S2. XPS spectra of N 1s region for (A) OH surface and (B) S-Glcp surface

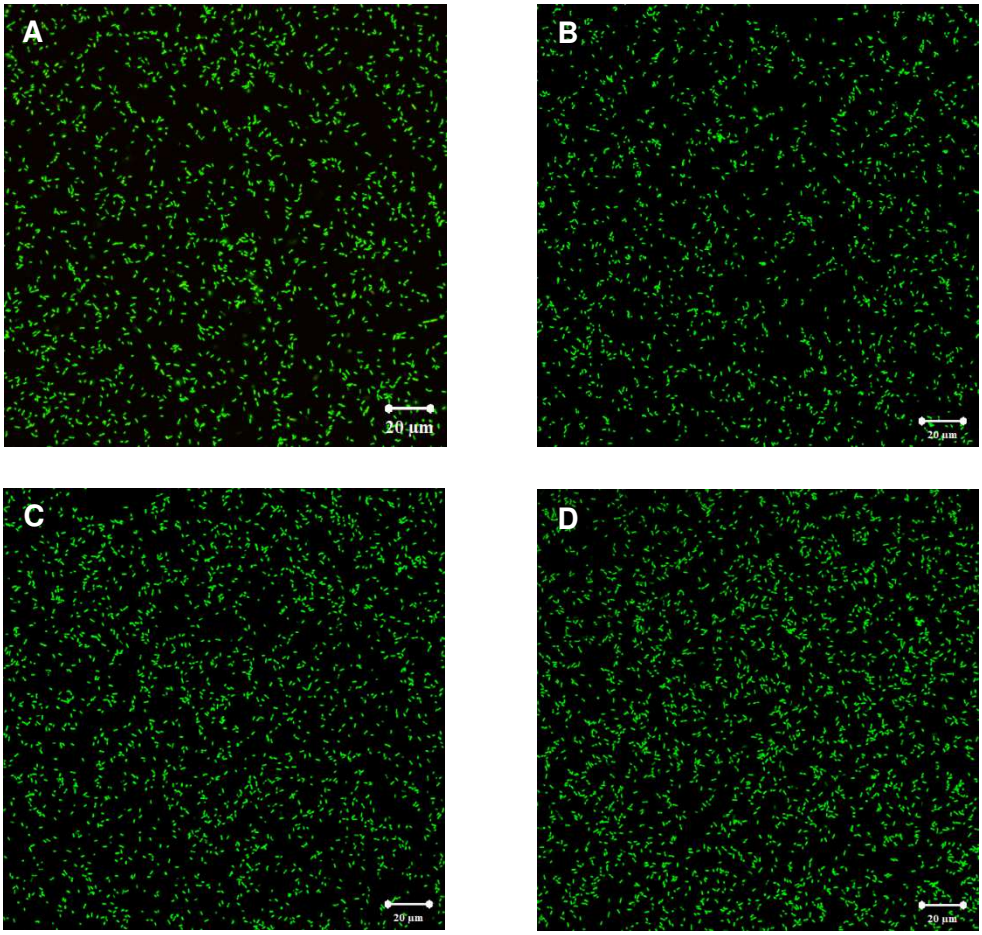

Figure S3. Microscopy images of adhered MPAO1 on *O*-D-galactopyranosidic (**A**), *O*-D-mannopyranosidic (**B**), *S*-D-galactopyranosidic (**C**) and *S*-D-mannopyranosidic surfaces (**D**)

Van Oss, Chaudhury and Good

The surface free energy for a solid (*s*) is divided into two components, the Lifshift-van der Waals (γ^{LW}) and the Lewis acid-base (γ^{AB}). The latter is dependent on the acid component γ_s^+ and the base component γ_s^- giving the relation:

$$\gamma_s = \gamma_s^{LW} + \gamma_s^{AB} = \gamma_s^{LW} + 2\sqrt{\gamma_s^- \gamma_s^+}$$

A combining rule from Young and Fawkes equation provides a relation between the interfacial free energy and the contact angle θ of a liquid (l) with the surface:

$$\gamma_l(1 + cos\,\theta) = 2\left(\sqrt{\gamma_s^{LW}\gamma_l^{LW}} + \sqrt{\gamma_s^+\gamma_l^-} + \sqrt{\gamma_s^-\gamma_l^+}\right)$$

Measuring the contact angle of a liquid with known surface free energy components leads to an equation with three unknown variables; $\gamma_l^{LW}, \gamma_l^+, \gamma_l^-$ (Table S1). To solve this, an equation system could be applied with three liquid with known components such as water (W), formamide (FA) and diiodomethane (DI):

$$\begin{cases} \gamma_W(1 + \cos\theta_W) = 2\left(\sqrt{\gamma_s^{LW}\gamma_W^{LW}} + \sqrt{\gamma_s^+\gamma_W^-} + \sqrt{\gamma_s^-\gamma_W^+}\right) \\ \gamma_{FA}(1 + \cos\theta_{DI}) = 2\left(\sqrt{\gamma_s^{LW}\gamma_{FA}^{LW}} + \sqrt{\gamma_s^+\gamma_{FA}^-} + \sqrt{\gamma_s^-\gamma_{FA}^+}\right) \\ \gamma_{DI}(1 + \cos\theta_{DI}) = 2\left(\sqrt{\gamma_s^{LW}\gamma_{DI}^{LW}} + \sqrt{\gamma_s^+\gamma_{DI}^-} + \sqrt{\gamma_s^-\gamma_{DI}^+}\right) \end{cases}$$

As Diiodomethane is an apolar solvent, the Lewis acid-base component γ_{DI}^{AB} is zero, then the system is simplify as following:

$$\begin{cases} \gamma_W(1 + \cos\theta_W) = 2\left(\sqrt{\gamma_s^{LW}\gamma_W^{LW}} + \sqrt{\gamma_s^+\gamma_W^-} + \sqrt{\gamma_s^-\gamma_W^+}\right) \\ \gamma_{FA}(1 + \cos\theta_{DI}) = 2\left(\sqrt{\gamma_s^{LW}\gamma_{FA}^{LW}} + \sqrt{\gamma_s^+\gamma_{FA}^-} + \sqrt{\gamma_s^-\gamma_{FA}^+}\right) \\ \gamma_s^{LW} = \dfrac{(\gamma_{DI}(1 + \cos\theta_{DI})^2}{4\gamma_{DI}^{LW}} \end{cases}$$

Table S1. Values of surface free energy components of solvents using for the determination of surface free energy and adhesion free energy.

	γ_l^{LW}	γ_l^+	γ_l^-	γ_l^{AB}	γ_l
Water (W)	21.8	25.5	25.5	51.0	72.8
Formamide (FA)	39.0	2.28	39.6	19.0	58.0
Diiodomethane (DI)	50.8	0	0	0	50.8

Table S2. Contact angle values used for the determination of surface free energy and adhesion free energy.

	Contact angles (°)		
	θ^W	θ^{FA}	θ^{DI}
Azide	75.6 ± 1.6	47.8 ± 1.1	34.5 ± 0.6
OH	67.8 ± 1.9	46.7 ± 1.1	42.0 ± 1.8
O-Glc*p*	56.5 ± 1.7	36.7 ± 0.8	37.4 ± 1.1
O-Gal*p*	56.3 ± 1.6	36.1 ± 1.1	38.2 ± 1.8
O-Man*p*	56.4 ± 1.9	34.3 ± 0.9	38.5 ± 1.3
S-Glc*p*	57.9 ± 1.9	35.7 ± 1.2	38.6 ± 1.4
S-Gal*p*	57.0 ± 1.8	35.8 ± 1.0	38.8 ± 2.2
S-Man*p*	57.1 ± 1.5	33.8 ± 1.1	37.3 ± 2.0
MPAO1	26.2 ± 2.1	34.8 ± 2.7	87.2 ± 1.4

References

[1] A.L.M. Morotti, K.L. Lang, I. Carvalho, E.P. Schenkel, L.S.C. Bernardes, Semi-Synthesis of new glycosidic triazole derivatives of dihydrocucurbitacin B, Tetrahedron Lett. 56 (2015) 303–307. doi:10.1016/j.tetlet.2014.11.049.

[2] N. Pietrzik, C. Schips, T. Ziegler, Efficient synthesis of glycosylated asparaginic acid building blocks via click chemistry, Synthesis (Stuttg). (2008) 0519–0526. doi:10.1055/s-2008-1032150.

[3] M. Lo Conte, S. Staderini, A. Marra, M. Sanchez-Navarro, B.G. Davis, A. Dondoni, Multi-molecule reaction of serum albumin can occur through thiol-yne coupling, Chem. Commun. 47 (2011) 11086. doi:10.1039/c1cc14402b.

[4] D. Giguère, M.A. Bonin, P. Cloutier, R. Patnam, C. St-Pierre, S. Sato, R. Roy, Synthesis of stable and selective inhibitors of human galectins-1 and -3, Bioorganic Med. Chem. 16 (2008) 7811–7823. doi:10.1016/j.bmc.2008.06.044.

[5] R. Lanzetta, A.M. Marzaioli, M. Parrilli, C. De Castro, E. Bedini, Conversion of yeast mannan polysaccharide in mannose oligosaccharides with a thiopropargyl linker at the pseudo-reducing end, Carbohydr. Res. 383 (2013) 43–49. doi:10.1016/j.carres.2013.10.016.

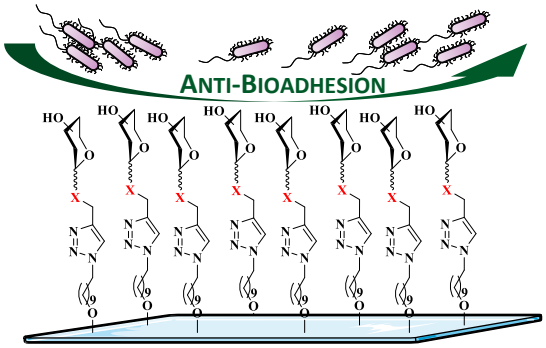
ANTI-BIOADHESION